Metabolic Engineering 36 (2016) 99–115

Contents lists available at ScienceDirect

Metabolic Engineering

journal homepage: www.elsevier.com/locate/ymben

Review

Engineering cytosolic acetyl-coenzyme A supply in *Saccharomyces cerevisiae*: Pathway stoichiometry, free-energy conservation and redox-cofactor balancing

Harmen M. van Rossum, Barbara U. Kozak, Jack T. Pronk, Antonius J.A. van Maris *

Department of Biotechnology, Delft University of Technology, Julianalaan 67, 2628 BC Delft, The Netherlands

ARTICLE INFO

Article history:
Received 30 January 2016
Received in revised form
20 March 2016
Accepted 21 March 2016
Available online 23 March 2016

Keywords:
Acetylating acetaldehyde dehydrogenase
Pyruvate-formate lyase
Pyruvate dehydrogenase
ATP-citrate lyase
Phosphoketolase
Carnitine shuttle

ABSTRACT

Saccharomyces cerevisiae is an important industrial cell factory and an attractive experimental model for evaluating novel metabolic engineering strategies. Many current and potential products of this yeast require acetyl coenzyme A (acetyl-CoA) as a precursor and pathways towards these products are generally expressed in its cytosol. The native *S. cerevisiae* pathway for production of cytosolic acetyl-CoA consumes 2 ATP equivalents in the acetyl-CoA synthetase reaction. Catabolism of additional sugar substrate, which may be required to generate this ATP, negatively affects product yields. Here, we review alternative pathways that can be engineered into yeast to optimize supply of cytosolic acetyl-CoA as a precursor for product formation. Particular attention is paid to reaction stoichiometry, free-energy conservation and redox-cofactor balancing of alternative pathways for acetyl-CoA synthesis from glucose. A theoretical analysis of maximally attainable yields on glucose of four compounds (*n*-butanol, citric acid, palmitic acid and farnesene) showed a strong product dependency of the optimal pathway configuration for acetyl-CoA synthesis. Moreover, this analysis showed that combination of different acetyl-CoA production pathways may be required to achieve optimal product yields. This review underlines that an integral analysis of energy coupling and redox-cofactor balancing in precursor-supply and product-formation pathways is crucial for the design of efficient cell factories.

Contents

Abbreviations: A-ALD, acetylating acetaldehyde dehydrogenase; acetyl-CoA, acetyl coenzyme A; acetyl-P, acetyl-phosphate; Ach1, CoA-transferase; ACL, ATP-citrate lyase; ACS, acetyl-CoA synthetase; ADH, alcohol dehydrogenase; ALD, acetaldehyde dehydrogenase; CAT, carnitine acetyltransferase; CIT, citrate synthase; CoA, coenzyme A; E(rythrose-)4P, erythrose-4-phosphate; F1,6P, fructose-1,6-biphosphate; F6P, fructose-6-phosphate; FDH, formate dehydrogenase; FeS, iron-sulfur; FPR, flavodoxin-NADP+ reductase; fructose-6-P, fructose-6-phosphate; G(lyceraldehyde-)3P, glyceraldehyde-3-phosphate; LSC, succinyl-CoA ligase; P, phosphate; P_i, inorganic phosphate; PDC, pyruvate decarboxylase; PDH, pyruvate dehydrogenase; PDH bypass, pyruvate dehydrogenase bypass; PFL, pyruvate-formate lyase; PFO, pyruvate-ferredoxin/flavodoxin oxidoreductase; PK, phosphoketolase; POX, pyruvate oxidase; PP_i, pyrophosphate; PTA, phosphotransacetylase; R(ibose-)5-P, ribose-5-phosphate; Ribulose-5-P, ribulose-5-phosphate; S7P, sedoheptulose-7-phoshate; TCA, tricarboxylic acid; TPP, thiamine pyrophosphate; X(ylulose-)5P, xylulose-5-phosphate; γ, degree of reduction; γ_P, degree of reduction of product; γ_S, degree of reduction of substrate; $\Delta G_R^{\circ\prime}$, the change in Gibbs free energy at pH=7 and an ionic strength of 100 mM and 1 M concentrations of reactants

* Corresponding author.
E-mail address: A.J.A.vanMaris@tudelft.nl (A.J.A. van Maris).

http://dx.doi.org/10.1016/j.ymben.2016.03.006
1096-7176/

1. Introduction

Over the past decades, the yeast *Saccharomyces cerevisiae* has become an important, multi-purpose cell factory (Nielsen, 2014; Nielsen et al., 2013). Its popularity is and continues to be stimulated by a large body of knowledge on yeast physiology and by fast developments in yeast molecular genetics, genomics and systems biology. A myriad of product pathways introduced into *S. cerevisiae* now enable the synthesis, from simple sugars, of products as diverse as benzylisoquinoline alkaloids (DeLoache et al., 2015), C_4-alcohols (Avalos et al., 2013; Branduardi et al., 2013; Steen et al., 2008), flavonoids (Koopman et al., 2012), isoprenoids (Beekwilder et al., 2014; Verwaal et al., 2007), organic acids (Miller et al., 2011; Porro et al., 1995; Van Maris et al., 2004b; Zelle et al., 2008) and fatty acids (Choi and Da Silva, 2014).

Acetyl coenzyme A (acetyl-CoA), an essential molecule in all known life forms (Kanehisa et al., 2014), is a key precursor for many compounds whose production by *S. cerevisiae* has been made possible by metabolic engineering. Examples include *n*-butanol (Krivoruchko et al., 2013), (poly)hydroxybutyrate (Kocharin et al., 2013; Leaf et al., 1996), fatty acids and derived compounds (Choi and Da Silva, 2014), isoprenoids such as β-carotene (Verwaal et al., 2007), farnesene (Sandoval et al., 2014) and artemisinic acid (Paddon et al., 2013) and flavonoids such as naringenin (Koopman et al., 2012). In native yeast metabolism, acetyl-CoA is required for synthesis of amino acids (e.g. leucine, arginine, methionine and cysteine), fatty acids, sterols, glutathione, *N*-acetylglucosamine and *S*-adenosyl-methionine (Kanehisa et al., 2014; Oura, 1972). Moreover, acetyl-CoA acts as acetyl donor for protein acetylation (Galdieri et al., 2014; Pokholok et al., 2005) and as an effector of enzymes (e.g. pyruvate carboxylase; Gailiusis et al., 1964; Ruiz-Amil et al., 1965).

In biotechnological processes for production of commodity chemicals from carbohydrates, costs of the feedstock may contribute up to 75% of the total costs (Lynd et al., 1999). In such cases, process economy dictates that product yields on substrate should approximate the theoretical maxima defined by elemental conservation laws and thermodynamics (Cueto-Rojas et al., 2015). To avoid excessive biomass formation, while still fulfilling energy requirements for cellular maintenance, product formation should ideally lead to a low but positive net ATP gain. Furthermore, processes should preferably be anaerobic, to maximize product yields and eliminate costs for oxygenation of large reactors. Even when thermodynamic- or biochemical constraints demand oxygen consumption, product yields on oxygen should be maximized, for example by eliminating ATP-requiring reactions in product formation. In view of these generic optimization criteria, ATP stoichiometry, carbon conservation and redox-cofactor balancing strongly affect process economy in microbial production processes (De Kok et al., 2012; Weusthuis et al., 2011).

The eukaryote *S. cerevisiae* uses dedicated mechanisms to meet acetyl-CoA requirements in its different subcellular compartments (Krivoruchko et al., 2015), of which the cytosolic and mitochondrial compartments are especially relevant for industrial product formation by this yeast. Since the inner mitochondrial membrane is impermeable to acetyl-CoA, mitochondrial acetyl-CoA cannot be directly exported to the cytosol (Flikweert et al., 1999; Van den Berg and Steensma, 1995). This compartmentation of acetyl-CoA metabolism directly affects cellular energetics since, in terms of ATP stoichiometry, the mitochondrial pyruvate-dehydrogenase (PDH) complex is superior to the PDH bypass pathway for cytosolic acetyl-CoA synthesis (Table 1; Pronk et al., 1994). Directly connecting a heterologous or synthetic product pathway to the mitochondrial acetyl-CoA pool would therefore require targeting of pathway enzymes to the mitochondrial matrix. Moreover, extensive engineering would be required to enable efficient mitochondrial transport of pathway intermediates, products and/or cofactors. So far, only few studies have explored functional expression of heterologous product pathways in yeast mitochondria (Avalos et al., 2013; Farhi et al., 2011). Instead, product pathways are commonly expressed in the yeast cytosol and, therefore, dependent on the cytosolic acetyl-CoA pool. Since the nuclear envelope is permeable for small molecules such as acetyl-CoA, the nucleosol, in which important histone acetylation reactions occur, is implicitly included in the cytosol throughout this review.

Recent publications have reviewed the roles of acetyl-CoA in yeast metabolism (Krivoruchko et al., 2015), yeast metabolic engineering (Krivoruchko et al., 2015; Lian and Zhao, 2015a; Sheng and Feng, 2015) and yeast cellular regulation (Galdieri et al., 2014). The present review focuses on aspects of metabolic engineering of acetyl-CoA metabolism in *S. cerevisiae* that goes beyond the scope of these previous papers. In particular, we systematically evaluate ATP stoichiometry, carbon conservation and redox-cofactor requirements of different native and engineered cytosolic acetyl-CoA forming pathways and of shuttle mechanisms that may be used to transport mitochondrial acetyl-moieties to the yeast cytosol. To analyze the product dependency of optimum pathway configurations for precursor supply, the reviewed cytosolic acetyl-CoA supplying pathways are quantitatively evaluated in terms of maximally attainable yields on substrate and oxygen of four industrially relevant compounds: (i) *n*-butanol, (ii) citric acid, (iii) palmitic acid and (iv) farnesene. Additionally, thermodynamic and kinetic aspects of the alternative pathways are discussed. Although we focus on acetyl-CoA as a precursor in *S. cerevisiae*, the concepts

Table 1
Overall stoichiometry for formation from glucose of one mole of cytosolic acetyl-CoA for the native yeast *S. cerevisiae* PDH bypass pathway and for various alternative routes based on heterologous enzyme activities. Routes with the same overall stoichiometries are presented together.

Native yeast PDH bypass (via AMP-forming acetyl-CoA synthetase)

$\frac{1}{2}$ glucose + 2 $NAD(P)^+$ + ATP + CoA + H_2O → acetyl-CoA + 2 ($NAD(P)H + H^+$) + CO_2 + ADP + P_i

PDH bypass (via ADP-forming acetyl-CoA synthetase)

$\frac{1}{2}$ glucose + 2 $NAD(P)^+$ + CoA → acetyl-CoA + 2 ($NAD(P)H + H^+$) + CO_2

Phosphoketolase and phosphotransacetylase

$\frac{1}{3}$ glucose + $\frac{1}{3}$ ATP + CoA → acetyl-CoA + $\frac{1}{3}$ (ADP + P_i) + $\frac{2}{3}$ H_2O

ATP-independent oxidative conversion from pyruvate to acetyl-CoA (via A-ALD; PDH_{cyt}; PFL with FDH; or PDH_{mit} with carnitine shuttle)

$\frac{1}{2}$ glucose + 2NAD^+ + ADP + P_i + CoA → acetyl-CoA + 2($NADH + H^+$) + CO_2 + ATP + H_2O

Pyruvate oxidase

$\frac{1}{2}$ glucose + NAD^+ + ADP + P_i + CoA + $\frac{1}{2}$ O_2 → acetyl-CoA + NADH + H^+ + CO_2 + ATP + $2H_2O$

Citrate-oxaloacetate shuttle with ACL; or Ach1 with succinyl-CoA ligase and ACS

$\frac{1}{2}$ glucose + 2NAD^+ + CoA → acetyl-CoA + 2($NADH + H^+$) + CO_2

Abbreviations: acetyl-CoA, acetyl coenzyme A; A-ALD, acetylating acetaldehyde dehydrogenase; Ach1, coA-transferase; ACL, ATP-citrate lyase; ACS, acetyl-CoA synthethase; ALD, acetaldehyde dehydrogenase; CoA, coenzyme A; FDH, formate dehydrogenase; PDH_{cyt}, cytosolic pyruvate dehydrogenase; PDH_{mit}, mitochondrial pyruvate dehydrogenase; PFL, pyruvate-formate lyase.

discussed herein are also applicable to other precursors and microorganisms.

2. Reaction stoichiometries of pathways for cytosolic acetyl-CoA supply

2.1. Native pathway in glucose-grown S. cerevisiae: the PDH bypass

Prokaryotes generally produce acetyl-CoA from glucose via pathways that do not involve a net hydrolysis of ATP. Instead, most eukaryotic pathways for cytosolic acetyl-CoA synthesis have a higher ATP expenditure. In *S. cerevisiae*, the native pathway for cytosolic acetyl-CoA synthesis from pyruvate consist of pyruvate decarboxylase (PDC; EC 4.1.1.1), NAD^+-or $NADP^+$-dependent acetaldehyde dehydrogenase (ALD; EC 1.2.1.3 (NAD^+-dependent), EC 1.2.1.4 ($NADP^+$-dependent)) and the ATP-requiring reaction catalyzed by acetyl-CoA synthetase (ACS; EC 6.2.1.1). These reactions are collectively referred to as the pyruvate-dehydrogenase bypass (PDH bypass; Fig. 1A) (Pronk et al., 1996). ACS catalyzes activation of acetate with the concomitant hydrolysis of ATP to AMP and PP_i:

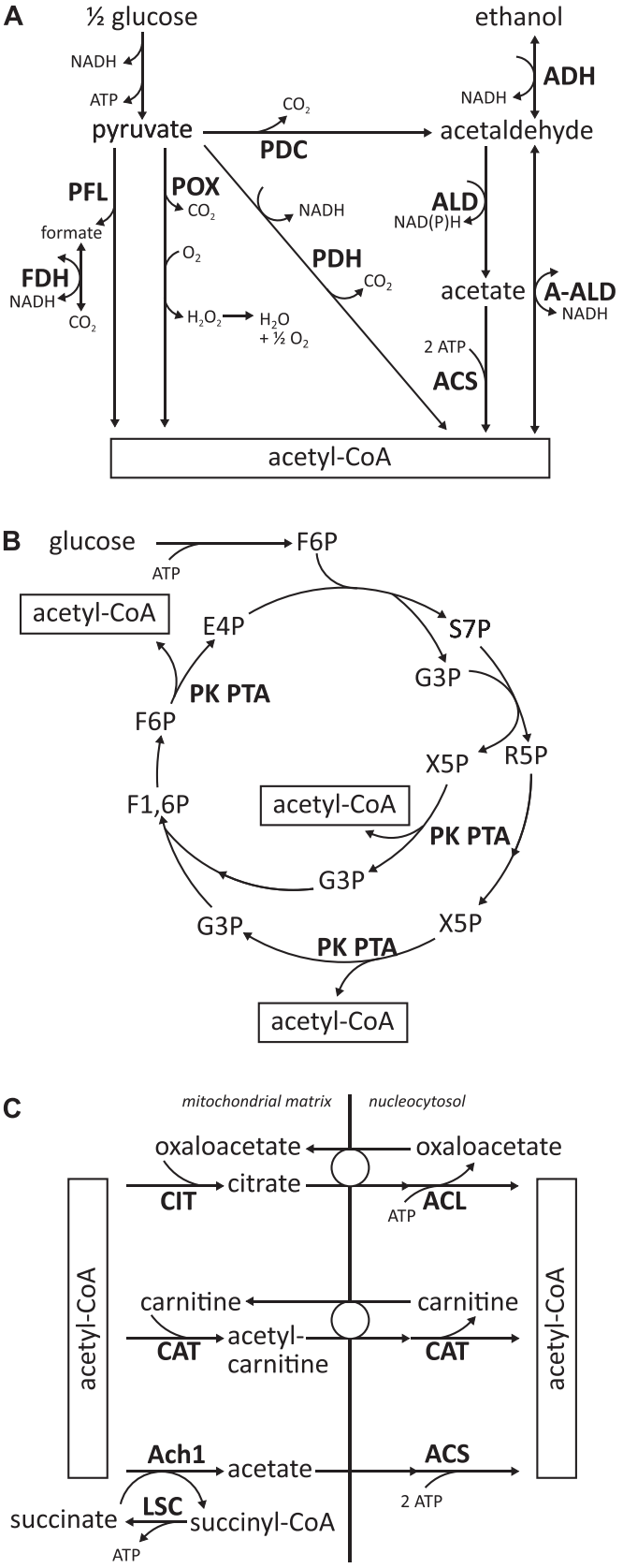

Fig. 1. Schematic representation of alternative routes for formation of acetyl-CoA in the cytosol of *Saccharomyces cerevisiae* **A** native PDH bypass; engineered pyruvate oxidase; pyruvate-formate lyase and formate dehydrogenase; pyruvate dehydrogenase; and acetylating acetaldehyde dehydrogenase. **B** One possible configuration of acetyl-CoA formation via phosphoketolase/-transacetylase in combination with pentose-phosphate-pathway enzymes, fructose-1,6-bisphosphatase and glycolysis (figure adapted from Bogorad et al. (2013)). **C** Shuttle mechanisms that result in net export of acetyl moieties from the mitochondrial matrix to the cytosol: citrate-oxaloacetate shuttle; carnitine shuttle; and mitochondrial formation of acetate by Ach1 followed by export to the cytosol. Abbreviations: acetyl-CoA, acetyl coenzyme A; A-ALD, acetylating acetaldehyde dehydrogenase; Ach1, CoA-transferase; ACL, ATP-citrate lyase; ACS, acetyl-CoA synthethase; ADH, alcohol dehydrogenase; ALD, acetaldehyde dehydrogenase; CAT, carnitine acetyltransferase; CIT, citrate synthase; E4P, erythrose-4-phosphate; F1,6P, fructose-1,6-bisphosphate; F6P, fructose-6-phosphate; FDH, formate dehydrogenase; G3P, glyceraldehyde-3-phosphate; LSC, succinyl-CoA ligase; PDC, pyruvate decarboxylase; PDH, pyruvate dehydrogenase complex; PFL, pyruvate-formate lyase; PK, phosphoketolase; POX, pyruvate oxidase; PTA, phosphotransacetylase; R5P, ribose-5-phosphate; S7P, sedoheptulose-7-phoshate; X5P, xylulose-5-phosphate.

$$\text{acetate} + \text{ATP} + \text{CoA} = \text{acetyl-CoA} + \text{AMP} + \text{PP}_i. \quad (1)$$

When activation of acetate by ACS is followed by the reactions catalyzed by pyrophosphatase (EC 3.6.1.1) and adenylate kinase (EC 2.7.4.3), the overall reaction sequence involves the net hydrolysis of 2 ATP to 2 ADP and 2 P_i. Involvement of pyrophosphatase has a strong impact on the overall thermodynamics of acetate activation. Reaction (1) has an estimated $\Delta G_R^{\circ\prime}$ of −4.5 kJ mol^{-1} (Flamholz et al., 2012), which decreases to −20.3 kJ mol^{-1} (Flamholz et al., 2012) when the pyrophosphatase reaction is included, thus enabling this essential biosynthetic reaction to function *in vivo* at a wide range of concentrations of its substrates and products.

Stoichiometrically, formation of 1 acetyl-CoA from glucose through glycolysis and PDH bypass requires 1 ATP and results in the net formation of 2 NADH or 1 NADH and 1 NADPH (Table 1). ATP required for cytosolic acetyl-CoA synthesis has to be generated by dissimilation of glucose through respiratory or fermentative dissimilation of glucose. This ATP requirement for precursor supply can severely limit the maximum attainable yields on glucose of cytosolic acetyl-CoA-derived products by *S. cerevisiae*.

2.2. Heterologous pathways for cytosolic acetyl-CoA supply

To decrease ATP costs for cytosolic acetyl-CoA supply, alternative (heterologous) pathways that convert glucose into cytosolic acetyl-CoA can be considered for functional replacement of the PDH bypass. For example, one might consider replacing the native *S. cerevisiae* ACS by a heterologous ADP-forming acetyl-CoA synthetase (EC 6.2.1.13), which catalyzes the conversion of acetate and ATP to acetyl-CoA and ADP:

$$\text{acetate} + \text{ATP} + \text{CoA} = \text{acetyl-CoA} + \text{ADP} + \text{P}_i. \quad (2)$$

This apparently simple replacement would make formation of acetyl-CoA from glucose an ATP-neutral process, while still generating 2 mol of NAD(P)H per mole of acetyl-CoA (Table 1). However, with an estimated $\Delta G_R^{\circ\prime}$ of +3.6 kJ mol^{-1} (Flamholz et al., 2012), use of ADP-forming ACS as an acetyl-CoA generating reaction poses strict requirements on the concentrations of intracellular substrate and product concentrations. To our knowledge, ADP-forming acetyl-CoA synthetases have not yet been functionally expressed in yeast.

In this section, six additional heterologous acetyl-CoA supplying routes are discussed in terms of their ATP- and redox-cofactor stoichiometry and with respect to their functional expression in *S. cerevisiae*. Five of these routes, relying on phosphoketolase/-transacetylase, acetylating acetaldehyde dehydrogenase, pyruvate-formate lyase, pyruvate dehydrogenase and pyruvate oxidase (Fig. 1A and B), have already been implemented in *S. cerevisiae*. A sixth, based on pyruvate-ferredoxin/flavodoxin oxidoreductase, has not yet been expressed in yeast.

2.2.1. Phosphoketolase and phosphotransacetylase

Phosphoketolase (PK; EC 4.1.2.9 and EC 4.1.2.22) and phosphotransacetylase (PTA; EC 2.3.1.8) are involved in the central carbon metabolism of heterofermentative lactic acid bacteria and in some fungi (Evans and Ratledge, 1984; Kandler, 1983). PK enzymes can use either fructose-6-P, xylulose-5-P or ribulose-5-P as substrates (Heath et al., 1958; Schramm et al., 1958) and differ with respect to their specificities for these three substrates (Chang et al., 2014; Heath et al., 1958; Schramm et al., 1958). PK converts these sugar phosphates and inorganic phosphate into acetyl-P and either erythrose-4-P or glyceraldehyde-3-P:

$$\text{fructose-6-P} + \text{P}_i = \text{acetyl-P} + \text{erythrose-4-P} + \text{H}_2\text{O}, \quad (3)$$

$$\text{xylulose-5-P} + \text{P}_i = \text{acetyl-P} + \text{glyceraldehyde-3-P} + \text{H}_2\text{O}, \quad (4)$$

$$\text{ribulose-5-P} + \text{P}_i = \text{acetyl-P} + \text{glyceraldehyde-3-P} + \text{H}_2\text{O}. \quad (5)$$

The acetyl-P formed in Reactions (3)–(5), which are all exergonic under biochemical standard conditions (estimated $\Delta G_R^{\circ\prime} = -49.9$ to -63.2 kJ mol^{-1}; Flamholz et al., 2012), can subsequently be converted to acetyl-CoA by the reversible PTA reaction (Stadtman, 1952; estimated $\Delta G_R^{\circ\prime} = -9.8$ kJ mol^{-1} in the acetyl-CoA forming direction; Flamholz et al., 2012):

$$\text{acetyl-P} + \text{CoA} = \text{acetyl-CoA} + \text{P}_i. \quad (6)$$

Schramm and Racker (1957) postulated that concerted action of PK, enzymes of the non-oxidative part of the pentose-phosphate pathway, glycolysis and the gluconeogenic enzyme, fructose-1,6-bisphosphatase (FBPase; EC 3.1.3.11), could catalyze conversion of 1 mole of fructose-6-P, without carbon loss, into 3 moles of acetyl-P (Fig. 1B), according to the following net reaction:

$$\text{fructose-6-P} + 2\text{P}_i = 3\ \text{acetyl-P} + 2\ \text{H}_2\text{O}. \quad (7)$$

Reaction (7) is strongly exergonic (estimated $\Delta G_R^{\circ\prime} = -302.2$ kJ mol^{-1}; Flamholz et al., 2012), suggesting that it should operate when the required enzymes are simultaneously present. Indeed, Schramm et al. (1958) observed a yield of acetate on fructose-6-P in cell extracts of *Acetobacter xylinum* that was consistent with the operation of this so-called fructose-6-P shunt. Over half a century later, conversion of fructose-6-P to acetyl-P without carbon loss was 'rediscovered' (Bogorad et al., 2013), this time in a reconstituted *in vitro* enzyme system. Subsequent expression of *Bifidobacterium adolescentis* PK and overexpression of FBPase in an engineered *E. coli* strain enabled anaerobic conversion of xylose to acetate at a molar yield of 2.2 mol mol^{-1}. This stoichiometry is close to 2.5 mol mol^{-1}, the predicted yield for *in vivo* operation of the fructose-6-P shunt (Bogorad et al., 2013).

In theory, it should be possible to implement a full fructose-6-P shunt in *S. cerevisiae* (Fig. 1B) by expression of heterologous PK and PTA enzymes and bypassing the glucose repression of the yeast *FBP1* gene and glucose inactivation of the encoded FBPase (Gancedo, 1971; Gancedo and Gancedo, 1971). Provided that futile cycling as a result of the simultaneous presence of phosphofructokinase and FBPase (Navas and Gancedo, 1996) can be avoided, this strategy should enable formation of 1 mole of acetyl-CoA at the cost of only one-third of a mole of ATP, without involvement of redox cofactors (Table 1). The same stoichiometry for conversion of sugar to acetyl-CoA can be achieved in a cycle similar to the one shown in Fig. 1B, but with xylulose-5-P as the sole substrate for PK. When subsequent formation of a product from acetyl-CoA does not yield ATP, respiratory dissimilation of acetyl-CoA via the TCA-cycle or simultaneous operation of an alternative, ATP-yielding pathway for cytosolic acetyl-CoA synthesis will be required. Similarly, when product formation from acetyl-CoA requires NAD(P)H, electrons will have to be made available elsewhere in metabolism. PK can also be combined with acetate kinase (AK; EC 2.7.2.1; acetyl-P + ADP = acetate + ATP). The thus formed acetate can be used by ACS, yielding acetyl-CoA, albeit at a decreased ATP efficacy compared to PK/PTA.

While PK activity has been reported in wild-type strains of *S. cerevisiae* (Evans and Ratledge, 1984; Sonderegger et al., 2004; Thykaer and Nielsen, 2007), activities in cell extracts are low and the responsible gene has not been identified. Several studies have explored expression of heterologous PK and PTA or AK genes in *S. cerevisiae*. In a study on pentose fermentation, PK from *Bifidobacterium lactis* and PTA from *Bacillus subtilis* were successfully expressed in *S. cerevisiae*, as confirmed by enzyme assays (Sonderegger et al., 2004). Later studies combined expression of a heterologous PK with either expression of an AK from *Aspergillus*

nidulans or of a PTA from *B. subtilis* in order to improve production of fatty-acid ethyl esters and polyhydroxybutyrate by *S. cerevisiae* (De Jong et al., 2014; Kocharin et al., 2013). However, during growth on glucose, the flux through the PK pathway in these modified *S. cerevisiae* strains appeared to be low (De Jong et al., 2014; Kocharin et al., 2013). In patent literature, implementation of a PK/PTA pathway in yeast has been reported, combining the PK from *Leuconostoc mesenteroides* and PTA from *Clostridium kluyveri* (Hawkins et al., 2014) with a route towards the isoprenoid farnesene, whose synthesis requires 9 mol mol^{-1} of acetyl-CoA (Gardner et al., 2013; Hawkins et al., 2014).

2.2.2. Acetylating acetaldehyde dehydrogenase

Acetylating acetaldehyde dehydrogenase (A-ALD; EC 1.2.1.10) is involved in the C_2 metabolism of prokaryotes and catalyzes the following reversible reaction:

$$\text{acetaldehyde} + NAD^+ + CoA = \text{acetyl-CoA} + NADH + H^+. \quad (8)$$

Under biochemical standard conditions, the estimated $\Delta G_R^{\circ\prime}$ of this reversible reaction is -17 kJ mol^{-1} in the acetyl-CoA forming direction (Flamholz et al., 2012). In contrast to $NAD(P)^+$-dependent ALD and ACS (Fig. 1A; Table 1), which together catalyze the conversion of acetaldehyde to acetyl-CoA in the native PDH bypass, Reaction (8) does not require ATP. Conversion of glucose to acetyl-CoA via glycolysis, PDC and A-ALD yields 1 mole of ATP and 2 moles of NAD(P)H per mole of acetyl-CoA (Fig. 1A; Table 1). Thus, A-ALD provides metabolic engineers with an ATP-yielding option for the synthesis of cytosolic acetyl-CoA from glucose. Furthermore, in contrast to the PK/PTA pathway, this route also yields NADH.

Kozak et al. (2014a) demonstrated functional expression of five prokaryotic A-ALDs, originating from *E. coli* (mhpF and EutE), *Pseudomonas sp.* (dmpF), *Staphylococcus aureus* (adhE) and *Listeria innocua* (lin1129), in *S. cerevisiae*. Expression of A-ALD was shown to functionally complement inactivation of the native PDH bypass pathway for cytosolic acetyl-CoA synthesis (Kozak et al., 2014a), although biomass yields of the engineered strains were lower than expected (see below). The potential benefit of A-ALD on cellular energetics is even larger when ethanol is considered as (co-)substrate (Kozak et al., 2016). Ethanol metabolism by *S. cerevisiae* is initiated by its conversion to cytosolic acetyl-CoA through the concerted activity of alcohol dehydrogenase, ALD and ACS. In a theoretical analysis, Kozak et al. (2016) showed that replacing this native route by an engineered A-ALD-dependent route could potentially increase the biomass yield on ethanol by up to 40%. If this strategy can be functionally implemented, these ATP savings could make ethanol a much more attractive (co-)substrate for industrial production of acetyl-CoA derived molecules.

2.2.3. Pyruvate-formate lyase

Another reaction that yields acetyl-CoA from pyruvate is catalyzed by pyruvate-formate lyase (PFL; EC 2.3.1.54; Chantrenne and Lipmann, 1950):

$$\text{pyruvate} + CoA = \text{acetyl-CoA} + \text{formate}. \quad (9)$$

Reaction (9) has an estimated $\Delta G_R^{\circ\prime}$ of -21.2 kJ mol^{-1} (Flamholz et al., 2012) and plays a key role in fermentation pathways in a large number of anaerobic microorganisms (Dandekar et al., 1999; Stairs et al., 2011). The redox-cofactor stoichiometry of the formation of acetyl-CoA from glucose through PFL depends on the subsequent metabolic fate of formate. To obtain the highest possible electron efficacy and to avoid weak-organic-acid uncoupling by formate (Geertman et al., 2006; Overkamp et al., 2002), the formate produced by PFL has to be oxidized to CO_2, a reaction catalyzed by formate dehydrogenase (FDH; EC 1.2.1.2):

$$\text{formate} + NAD^+ = CO_2 + NADH + H^+. \quad (10)$$

Formation of acetyl-CoA from glucose through the combined action of PFL and NAD^+-dependent FDH yields 1 ATP and 2 NADH per acetyl-CoA, which is identical to the net stoichiometry of the A-ALD route described above (Fig. 1A; Table 1). Theoretically, application of PFL with or without FDH or together with a formate-hydrogen lyase (EC 1.1.99.33; Sawers, 1994), creates flexibility in metabolic engineering strategies that include these enzymes. Furthermore, protein engineering has yielded FDH enzymes that use $NADP^+$ instead of NAD^+ as a cofactor (Hoelsch et al., 2013; Serov et al., 2002). The latter option is of particular interest when product formation pathways downstream of acetyl-CoA use NADPH as the electron donor, as is for instance the case in fatty-acid synthesis. However, the biochemistry of PFL and, as will be discussed later, FDH represent significant challenges.

Catalytic activity of PFL depends on a radical residue, which is introduced by abstraction of a hydrogen atom from its active site by a specific PFL-activating enzyme (PFL-AE; EC 1.97.1.4). Activation of PFL by PFL-AE involves the flavoprotein flavodoxin (Knappe et al., 1969). In *E. coli*, flavodoxin is encoded by *fldA* and its reduction depends on the flavodoxin-$NADP^+$ reductase, encoded by *fpr* (McIver et al., 1998). Its radical residue makes PFL highly sensitive to molecular oxygen, which causes irreversible cleavage of PFL in two inactive fragments (Knappe et al., 1969). Moreover, also the essential [4Fe-4S] cluster in the active site of PFL-AE is oxygen labile (Külzer et al., 1998).

PFL and PFL-AE from *E. coli* were first expressed in *S. cerevisiae* by Waks and Silver (2009), who demonstrated formate accumulation during anaerobic growth of the resulting yeast strains. PFL was subsequently shown to functionally replace the native PDH bypass as the sole pathway for cytosolic acetyl-CoA synthesis in anaerobic *S. cerevisiae* cultures (Kozak et al., 2014a). Expression of PFL and PFL-AE from either *E. coli* or *Lactobacillus plantarum* supported anaerobic specific growth rates of an Acs^- strain of up to 73% of that of the Acs^+ reference strain. It is presently unclear which *S. cerevisiae* proteins functionally replace bacterial flavodoxins in these studies (Kozak et al., 2014a; Waks and Silver, 2009). Recently, co-expression of the flavodoxin:$NADP^+$ reductase system from *E. coli* was shown to enable PFL-dependent growth of engineered Pdc^- *S. cerevisiae* strains under microaerobic conditions (Y. Zhang et al., 2015b).

2.2.4. Pyruvate dehydrogenase complex

The pyruvate dehydrogenase (PDH) complex (EC 1.2.4.1, EC 2.3.1.12, EC 1.8.1.4) catalyzes the oxidative decarboxylation of pyruvate into acetyl-CoA:

$$\text{pyruvate} + NAD^+ + CoA = \text{acetyl-CoA} + CO_2 + NADH + H^+ \quad (11)$$

The estimated $\Delta G_R^{\circ\prime}$ of the overall reaction catalyzed by this multi-enzyme complex is -40.2 kJ mol^{-1} (Flamholz et al., 2012). Before the recent discovery of a nuclear PDH complex in human cells (Sutendra et al., 2014), eukaryotic PDH complexes were assumed to be confined to mitochondria, as is also the case in *S. cerevisiae* (Van den Berg and Steensma, 1995). Direct conversion of pyruvate to cytosolic acetyl-CoA via Reaction (11) therefore either requires relocalization of the native yeast mitochondrial PDH complex to the cytosol or cytosolic expression of a heterologous PDH complex. Stoichiometrically, formation of acetyl-CoA via a cytosolic PDH complex corresponds to the A-ALD or PFL/FDH-based pathways discussed above (Table 1). However, in contrast to these pathways, acetyl-CoA generation by the PDH complex does not involve the potentially toxic intermediates acetaldehyde or formate (Fig. 1A).

Functional expression of a heterologous PDH complex is complicated by its multi-subunit organization. The E1 subunit, in many

organisms consisting of separate E1α and E1β subunits, has pyruvate dehydrogenase activity (EC 1.2.4.1), E2 has dihydrolipoamide acetyltransferase activity (EC 1.2.4.1) and E3 has dihydrolipoyl dehydrogenase activity (EC 1.2.4.1) (Koike et al., 1963; Zhou et al., 2001). Multiple copies of each subunit assemble into a ~10 MDa complex (Snoep et al., 1992), which makes the whole complex larger than a yeast ribosome (Melnikov et al., 2012). Furthermore, the E2 subunit is only active when covalently linked to lipoic acid, which requires a specific lipoylation system (Cronan et al., 2005). As an additional complication, the E3 subunit of many PDH complexes is strongly inhibited by high [NADH]/[NAD^+] ratios. In most organisms, the PDH complex is therefore only active under aerobic conditions, when [NADH]/[NAD^+] ratios are lower than under anaerobic conditions (Bekers et al., 2015; Canelas et al., 2008; Snoep et al., 1992). However, the PDH complex from the Gram-positive bacterium *Enterococcus faecalis* was shown to exhibit a remarkably low sensitivity to high [NADH]/[NAD^+] ratios (Snoep et al., 1993), which enables it to function in its native host under anaerobic conditions (Snoep et al., 1992).

Functional expression and assembly of the *E. faecalis* PDH complex in the cytosol of *S. cerevisiae* was recently demonstrated (Kozak et al., 2014b). *In vivo* PDH activity not only required heterologous expression of the E1α, E1β, E2 and E3 subunits of *E. faecalis* PDH, but also of two *E. faecalis* genes involved in lipoylation of the E2 subunit and supplementation of growth media with lipoic acid. The *in vivo* activity of the cytosolic PDH-complex was sufficient to meet the cytosolic acetyl-CoA demand for growth, as demonstrated by complementation in Acs^- *S. cerevisiae* strains (Kozak et al., 2014b). Growth of these strains was also observed under anaerobic conditions, consistent with the previously reported ability of this PDH complex to operate at elevated [NADH]/[NAD^+] ratios (see above).

2.2.5. Pyruvate oxidase

In many prokaryotes, the flavoprotein pyruvate oxidase (POX; EC 1.2.3.3) catalyzes oxidative decarboxylation of pyruvate to acetyl-P and donates electrons to oxygen, thereby forming hydrogen peroxide (Lipmann, 1940; Tittmann et al., 2005):

$$\text{pyruvate} + P_i + O_2 = \text{acetyl-P} + CO_2 + H_2O_2. \quad (12)$$

Following this strongly exergonic reaction (estimated $\Delta G_R^{\circ\prime} = -163.8$ kJ mol^{-1}; Flamholz et al., 2012), acetyl-CoA can be formed from acetyl-P by PTA (Reaction (6)). Detoxification of hydrogen peroxide can, for example, occur via catalase (EC 1.11.1.6):

$$2\ H_2O_2 = O_2 + 2\ H_2O. \quad (13)$$

Formation of 1 acetyl-CoA from glucose via glycolysis, Reactions (12), (13) and PTA (Reaction (6)) consumes $\frac{1}{2}\ O_2$ and forms 1 NADH and ATP (Fig. 1A; Table 1). Compared to the ATP-independent oxidative conversions of pyruvate into acetyl-CoA (by A-ALD, PFL/FDH or PDH), the POX route requires oxygen and yields fewer reducing equivalents. There is as yet no scientific literature on implementation of the POX strategy for cytosolic acetyl-CoA supply in *S. cerevisiae*. However, a recent patent application reports that combined expression of POX from *Aerococcus viridans* with a PTA increased the specific growth rate of an *S. cerevisiae* strain in which the PDH bypass was inactivated by deletion of all three pyruvate-decarboxylase genes (Nielsen et al., 2015).

2.2.6. Pyruvate-ferredoxin/flavodoxin oxidoreductase

Similar to the PDH complex, pyruvate-ferredoxin/flavodoxin oxidoreductase (PFO; EC 1.2.7.1) catalyzes oxidative decarboxylation of pyruvate to acetyl-CoA (Ragsdale, 2003). However, unlike the NADH-yielding PDH reaction, PFO transfers electrons to ferredoxin or flavodoxin. The iron-sulfur-cluster-containing PFO is oxygen sensitive, which probably restricts its applicability to anaerobic conditions. In some organisms, including *Helicobacter pylori*, an $NADP^+$-flavodoxin oxidoreductase (FPR; EC 1.18.1.2) can transfer electrons from reduced flavodoxin to $NADP^+$, yielding NADPH (Hughes et al., 1998). Interestingly, the protist *Euglena gracilis* harbors a chimeric mitochondrial pyruvate-$NADP^+$ oxidoreductase (EC 1.2.1.51) protein, which integrates PFO and FPR activity (Inui et al., 1984a; Rotte et al., 2001). In these reactions, pyruvate is converted into acetyl-CoA via PFO or via PFO and FPR through, respectively, the following reactions:

$$\text{pyruvate} + \text{ferredoxin/flavodoxin (oxidized)} + \text{CoA} = \text{acetyl-CoA} + CO_2 + \text{ferredoxin/flavodoxin (reduced)}, \quad (14)$$

$$\text{pyruvate} + NADP^+ + \text{CoA} = \text{acetyl-CoA} + CO_2 + \text{NADPH} + H^+. \quad (15)$$

Reactions (14) and (15) both have negative $\Delta G_R^{\circ\prime}$ values (estimated at −23.6 (with ferredoxin as redox cofactor) and −32.9 kJ mol^{-1}, respectively; Flamholz et al., 2012). Application of PFO and/or PFR for yeast metabolic engineering would require efficient regeneration of the reduced co-factors. For optimal electron efficacy, this would require reductive reaction steps downstream of acetyl-CoA that re-oxidize either reduced ferredoxin/flavodoxin or NADPH, as has for instance been shown for the anaerobic conversion of glucose to wax esters by *E. gracilis* (Inui et al., 1984b). If this requirement can be met, the overall stoichiometric impact of these enzymes on product formation would be identical to that of PDH, but would expand flexibility with respect to redox-cofactor specificity.

2.3. Export of mitochondrial acetyl moieties to the cytosol via shuttle mechanisms

The six strategies discussed above rely on direct formation of acetyl-CoA in the yeast cytosol. Alternatively, cytosolic acetyl-CoA may be provided through mitochondrial, ATP-independent formation of acetyl-CoA via the native PDH complex using shuttle mechanisms. Three such mechanisms that, by a combination of enzyme-catalyzed reactions and transport steps, enable the net export of mitochondrial acetyl moieties to the cytosol, are discussed below: the citrate-oxaloacetate shuttle, the carnitine shuttle and a shuttle mechanism that relies on mitochondrial conversion of acetyl-CoA to acetate.

2.3.1. Citrate-oxaloacetate shuttle

The citrate-oxaloacetate shuttle uses oxaloacetate as a carrier molecule to transfer acetyl moieties across the mitochondrial membrane. This shuttle not only occurs in many higher eukaryotes, but also in oleaginous yeasts, where it provides cytosolic acetyl-CoA for lipid synthesis (Boulton and Ratledge, 1981). In the citrate-oxaloacetate shuttle, acetyl-CoA formed by the mitochondrial PDH complex first reacts with oxaloacetate in a reaction catalyzed by mitochondrial citrate synthase (EC 2.3.3.1; Fig. 1C). Citrate generated in this reaction is then exported from the mitochondria via antiport with oxaloacetate or malate (Brunengraber and Lowenstein, 1973). The acceptor molecule in this shuttle mechanism, oxaloacetate, is then regenerated by ATP-dependent cleavage of citrate, catalyzed by cytosolic ATP-citrate lyase (ACL; EC 2.3.3.8):

$$\text{citrate} + \text{ATP} + \text{CoA} = \text{acetyl-CoA} + \text{oxaloacetate} + \text{ADP} + P_i \quad (16)$$

Finally, antiport of cytosolic oxaloacetate with mitochondrial citrate enables a new cycle of the shuttle (Fig. 1C). As the ATP generated via glycolysis is hydrolyzed again in Reaction (16), formation of cytosolic acetyl-CoA from glucose via ACL is ATP neutral and results in formation of 1 NADH in the cytosol and 1 NADH in the mitochondria (Table 1). To maintain redox-cofactor balance,

NADH formed in the mitochondria should either be re-oxidized via respiration or, via involvement of mitochondrial redox shuttles (Bakker et al., 2001), be translocated to the cytosol to be reoxidized in a product formation pathway.

In contrast to oleaginous yeasts, *S. cerevisiae* does not contain ACL (Boulton and Ratledge, 1981). However, *S. cerevisiae* mitochondria do contain a functional citrate-α-ketoglutarate antiporter, encoded by *YHM2*, which also has activity with oxaloacetate (Castegna et al., 2010). Functional expression of ACL from *Arabidopsis thaliana* in *S. cerevisiae* was first demonstrated by *in vitro* enzyme assays (Fatland et al., 2002). Two subsequent studies investigated the impact of the citrate-oxaloacetate shuttle on production of acetyl-CoA derived compounds by *S. cerevisiae*. Tang et al. (2013) showed that expression of a murine ACL resulted in a 1.1–1.2 fold increase in fatty-acid content during stationary phase (Tang et al., 2013). Similarly, expression of ACL from *Yarrowia lipolytica* resulted in a 2.4 fold increase of the *n*-butanol yield on glucose in *S. cerevisiae* strains that co-expressed a heterologous, acetyl-CoA dependent pathway to *n*-butanol (Lian et al., 2014). In another study, expression of the ACL enzymes from *A. nidulans*, *Mus musculus*, *Y. lipolytica*, *Rhodosporidium toruloides* and *Lipomyces starkeyii* in *S. cerevisiae* demonstrated that the *A. nidulans* ACL resulted in 4.2–9.7 fold higher activity than the other ACLs (Rodriguez et al., 2016). By applying a push/pull/block strategy on an *S. cerevisiae* strain expressing the *A. nidulans* ACL, acetyl-CoA-dependent production of mevalonate was improved (Rodriguez et al., 2016).

ACL is also involved in another potentially interesting strategy for cytosolic acetyl-CoA formation. This strategy, which has hitherto only been partially successful in *E. coli*, relies on reversal of the glyoxylate cycle by introduction of several ATP-dependent steps (Mainguet et al., 2013). By combined expression of ATP-citrate lyase, malate thiokinase (EC 6.2.1.9; malate + CoA + ATP = malyl-CoA + ADP + P_i) and a malyl-CoA lyase (EC 4.1.3.24; malyl-CoA = acetyl-CoA + glyoxylate), this pathway should enable the *in vivo* conversion of succinate and malate to oxaloacetate and 2 acetyl-CoA (Mainguet et al., 2013). While further research is required before this strategy can be applied in metabolic engineering, it could enable efficient conversion of C_4 substrates to 2 acetyl-CoA, without loss of carbon in the form of CO_2. However, this high carbon conversion will be at the expense of ATP hydrolysis.

2.3.2. Carnitine shuttle

The carnitine shuttle, which uses the quaternary ammonium compound L-carnitine as a carrier molecule, enables transport of acyl moieties between eukaryotic organelles (Bieber, 1988). When acetyl-CoA is the substrate, the carnitine shuttle consists of cytosolic and mitochondrial carnitine acetyltransferases (EC 2.3.1.7), which transfer activated acetyl-CoA to L-carnitine and vice versa (Reaction (17)), as well as an acetyl-carnitine translocase in the inner mitochondrial membrane (Fig. 1C).

$$\text{L-carnitine} + \text{acetyl-CoA} = \text{acetyl-L-carnitine} + \text{CoA} \quad (17)$$

In *S. cerevisiae*, at least six proteins contribute to a functional carnitine shuttle. In contrast to many other eukaryotes, including mammals (Vax and Wanders, 2002) and the yeast *Candida albicans* (Strijbis et al., 2009), *S. cerevisiae* lacks the genetic information required for L-carnitine biosynthesis (Swiegers et al., 2001; Van Roermund et al., 1995). Operation of the carnitine shuttle in *S. cerevisiae* therefore depends on availability of exogenous L-carnitine, which is imported via the Hnm1 plasma-membrane transporter (Aouida et al., 2013). Expression of *HNM1* is regulated by the plasma-membrane-spanning protein Agp2 (Aouida et al., 2013; Van Roermund et al., 1999). *S. cerevisiae* harbors three carnitine acetyltransferases (Bieber, 1988), with different subcellular localizations: Cat2 is active in the peroxisomal and mitochondrial matrices (Elgersma et al., 1995), Yat1 is localized to the outer mitochondrial membrane (Schmalix and Bandlow, 1993) and Yat2 is a cytosolic protein (Huh et al., 2003; Koh et al., 2015; Swiegers et al., 2001). The inner mitochondrial membrane contains an acetyl-carnitine translocase, Crc1 (Franken et al., 2008; Kohlhaw and Tan-Wilson, 1977; Palmieri et al., 1999; Van Roermund et al., 1999).

All components of the carnitine shuttle catalyze reversible reactions. Transport of the acetyl moiety of acetyl-CoA from the mitochondria to the cytosol via the carnitine shuttle should therefore, at least theoretically, enable the formation of acetyl-CoA from glucose with the generation of 1 ATP and the formation of 1 NADH in the mitochondria and 1 NADH in the cytosol (Table 1). However, in *S. cerevisiae* strains that express the genes of the carnitine shuttle from their native promotors, the shuttle does not contribute to export of mitochondrial acetyl moieties during growth on glucose (Van Maris et al., 2003). To circumvent the glucose repression that occurs in wild-type *S. cerevisiae* (Elgersma et al., 1995; Kispal et al., 1991; Schmalix and Bandlow, 1993), Van Rossum et al. (2016b) recently constructed an *S. cerevisiae* strain in which all genes involved in the carnitine shuttle were constitutively expressed. Elimination of the PDH bypass in such a strain background, followed by laboratory evolution, yielded strains whose growth on glucose was dependent on L-carnitine supplementation (Van Rossum et al., 2016b). This result indicated that acquisition of specific mutations in the yeast genome indeed allows the carnitine shuttle to export mitochondrial acetyl units to the cytosol. While this study presented a first proof of concept, further research is necessary to explore the potential industrial relevance of the carnitine shuttle as an alternative mechanism for supplying acetyl-CoA in *S. cerevisiae*.

2.3.3. Mitochondrial conversion of acetyl-CoA to acetate through the CoA-transferase Ach1

Whereas acetyl-CoA cannot cross the mitochondrial membrane, acetate likely can (see below). Mitochondrial conversion of acetyl-CoA to acetate, followed by export of acetate from the mitochondria and its subsequent activation by cytosolic ACS, could constitute an alternative acetyl-CoA shuttle (Fig. 1C). In *S. cerevisiae*, mitochondrial release of acetate from acetyl-CoA is catalyzed by Ach1, which was originally characterized as a mitochondrial acetyl-CoA hydrolase (EC 3.1.2.1; Buu et al., 2003). Subsequent *in vitro* studies with purified protein showed that Ach1 is, in fact, a CoA-transferase that can also catalyze the transfer of the CoA group between various CoA esters and short-chain organic acids (Fleck and Brock, 2009). When Ach1 uses succinate and acetyl-CoA as substrates, this results in the following reversible reaction:

$$\text{succinate} + \text{acetyl-CoA} = \text{succinyl-CoA} + \text{acetate}. \quad (18)$$

The overall ATP cost (or yield) of formation of cytosolic acetyl-CoA through this system depends on the reactions by which acetate is formed. If acetate is formed by hydrolysis of mitochondrial acetyl-CoA, formation of cytosolic acetyl-CoA from glucose, involving the native ACS, through this route costs 1 ATP. This stoichiometry would not provide an energetic benefit over the native PDH bypass. However, if mitochondrial acetate is formed by a CoA-transfer reaction with succinate as CoA acceptor, one ATP can be recovered by subsequently regenerating succinate via succinyl-CoA ligase (EC 6.2.1.5; Przybyla-Zawislak et al., 1998):

$$\text{succinyl-CoA} + \text{ADP} + P_i = \text{succinate} + \text{ATP} + \text{CoA}. \quad (19)$$

In this scenario, formation of cytosolic acetyl-CoA from glucose via Ach1-catalyzed CoA-transfer is an ATP neutral process (Fig. 1C; Table 1). When combined with an ADP-forming ACS (see above), formation of acetyl-CoA from glucose via this pathway could even

result in a net yield of 1 mole of ATP per mole of acetyl-CoA. These three scenarios all result in the formation of 1 mole of cytosolic NADH and 1 mole of mitochondrial NADH per mole of acetyl-CoA produced from glucose.

Combination of Ach1 activity with export of acetate to the cytosol has recently been shown to enable cytosolic acetyl-CoA synthesis in *S. cerevisiae* strains in which the PDH bypass was impaired by deletion of the pyruvate decarboxylases *PDC1*, *PDC5* and *PDC6* (Chen et al., 2015). Such Pdc$^-$ strains become auxotrophic for externally added acetate (or other C_2 compounds) as substrate for the cytosolic acetyl-CoA synthase (Flikweert et al., 1999). After previous studies had shown that this auxotrophy can be overcome by either laboratory evolution or by introduction of a stable *MTH1* allele (Oud et al., 2012; Van Maris et al., 2004a), Chen et al. (2015) showed that the acquired acetate prototrophy relies on Ach1. In these strains, Ach1 releases acetate in the mitochondria that is subsequently transported to the cytosol and activated to acetyl-CoA by cytosolic Acs1 and/or Acs2 (Reaction (1)) (Chen et al., 2015). The *in vivo* capacity of Ach1 in glucose-grown cultures of *S. cerevisiae* is low (Van Rossum et al., 2016a) and insufficient to sustain fast growth of Pdc$^-$ strains in the absence of further modification or evolution (Oud et al., 2012). Therefore, to fully explore the potential stoichiometric benefits of this system for product formation, increasing pathway capacity should be a first priority.

3. Coupling of cytosolic acetyl-CoA forming pathways to product formation: a stoichiometric analysis

The cytosolic acetyl-CoA forming pathways discussed above differ with respect to their acetyl-CoA, ATP, NAD(P)H and CO_2 stoichiometries (Table 1). Pathways that further convert cytosolic acetyl-CoA into industrially relevant products can have different redox-cofactor and ATP requirements. Therefore, the design of metabolic engineering strategies for optimal integration of acetyl-CoA forming pathway(s) with product pathways requires *a priori* stoichiometric analysis. Important considerations for designing optimal pathway configurations include the theoretical maximum reaction stoichiometry, thermodynamic feasibility and compatibility with the native biochemistry of the (engineered) host organism.

The maximum theoretical yield (mole product per mole substrate, in the absence of growth) can be calculated without prior assumptions on pathway biochemistry and describes a situation in which all available electrons from the substrate end up in the product of interest. In this situation, which does not involve the use of external electron acceptors such as oxygen, the theoretical maximum molar reaction stoichiometry can be written as follows (Cueto-Rojas et al., 2015):

$$-\frac{\gamma_P}{\gamma_S}\text{substrate} + n_{CO_2}CO_2 + n_{H_2O}H_2O + n_{H^+}H^+ + 1\ \text{product} = 0.$$

In this equation, γ_P and γ_S represent the degree of reduction (in e-mol mol^{-1}) of the product and substrate (Heijnen et al., 1992). Molar stoichiometries of the other compounds (n_{co_2}, n_{H_2O} and n_{H+}) then follow from elemental and charge balances. The degree of reduction is defined as the number of electrons that are released when a chemical compound is completely converted to its most oxidized stable reference compound(s). For carbohydrates and other C-, H-and O-containing molecules, these oxidized reference compounds are H_2O, CO_2 and H^+ which, by convention, are assigned a γ-value of 0. This assignment results in the following γ-value for the elements and charges: H=1; C=4; O=−2; +=−1; −=+1. The degree of reduction of any compound can then be simply calculated from the sum of the γ-values of its elements.

A first indication of whether a reaction is thermodynamically feasible is provided by its Gibbs free energy change under biochemical standard conditions ($\Delta G_R^{\circ\prime}$), taking into account that actual *in vivo* values of ΔG_R also depend on concentrations of substrates and products. In addition, $\Delta G_R^{\circ\prime}$ provides valuable indications on whether the Gibbs-free energy change is sufficiently negative to conserve free energy in the form of ATP for growth and cellular maintenance and to provide the thermodynamic driving force required for high reaction rates (Cueto-Rojas et al., 2015). When experimental data on the free energy of formation ($\Delta_f G^\circ$) of relevant compounds are not available, $\Delta G_R^{\circ\prime}$ estimations can instead be based on group contribution methods (Flamholz et al., 2012; Noor et al., 2013). If the theoretical maximum stoichiometry calculated via the degree-of-reduction approach is thermodynamically feasible, it represents the ultimate benchmark for assessment of alternative pathway configurations during the design phase of metabolic engineering projects.

Challenges in experimentally approaching maximum theoretical product yields by metabolic engineering are to a large extent caused by constraints that are imposed by the native biochemistry of microbial production hosts and/or by its (in)compatibility with relevant heterologous and/or synthetic pathways for precursor supply and product formation. For example, involvement of ATP-requiring reactions or non-matching redox-cofactor specificities of oxidative and reductive reactions in a pathway can constrain the experimentally attainable product yield. Optimally choosing or (re) designing pathway configurations in (central) metabolism is therefore crucial for systematically approaching the theoretical production yield.

To evaluate product dependency of the optimal reconfiguration of cytosolic acetyl-CoA provision in yeast, we evaluate the alternative pathways discussed above for the production of four model compounds: *n*-butanol, citric acid, palmitic acid and farnesene. This analysis is based on a compartmentalized model of central metabolism described by Carlson et al. (2002), supplemented with (heterologous) reactions for acetyl-CoA formation, the lumped reaction pathways from acetyl-CoA to the four products, as well as some additional modifications (Box 1).

3.1. n-Butanol

n-Butanol, a linear 4-carbon alcohol, is a promising renewable transport fuel as well as an industrial solvent and precursor for chemical synthesis (Mascal, 2012), with a maximum theoretical yield on glucose of 1 mol mol^{-1} (Table 2). While various pathways to *n*-butanol have been expressed in *S. cerevisiae* (Branduardi et al., 2013; Lian et al., 2014; Steen et al., 2008; Swidah et al., 2015), only the *Clostridium* pathway has acetyl-CoA as a precursor and is therefore considered in this review (Fig. 2A). This pathway has the following reaction stoichiometry:

$$2\text{acetyl-CoA} + 4(\text{NADH} + H^+) = n\text{-butanol} + 4\text{NAD}^+ + 2\text{CoA} + H_2O. \quad (20)$$

All four pathways for acetyl-CoA production can result in redox-cofactor balanced formation of butanol from glucose (Table 2). For the three routes that produce acetyl-CoA from glucose via pyruvate, the 4 NADH required for synthesis of 1 *n*-butanol are produced by glycolysis and by the subsequent oxidative conversion of pyruvate to acetyl-CoA. In the PK/PTA pathway, non-oxidative conversion of $\frac{2}{3}$ glucose to 2 acetyl-CoA requires, in parallel, the oxidation of $\frac{1}{3}$ glucose via glycolysis and TCA cycle to generate these 4 NADH. Deriving NADH from the TCA cycle will require additional metabolic engineering to overcome the subcellular compartmentation of NADH metabolism in *S. cerevisiae* (Bakker et al., 2001) and the down-regulation of TCA-cycle enzymes in anaerobic *S. cerevisiae*

Box 1–Modifications to the *Saccharomyces cerevisiae* stoichiometric model of Carlson et al (2002), introduced to enable stoichiometric comparison of different cytosolic acetyl-CoA forming pathways in the context of the production of *n*-butanol, citric acid, palmitic acid or farnesene (for complete model in MetaTool format (Von Kamp and Schuster, 2006), see Supplementary data 1).

- Based on experimental data (Van Maris et al., 2003; Van Rossum et al., 2016b), transport of mitochondrial acetyl-CoA to the cytosol was removed from the model.
- Introduction of reactions for formation of *n*-butanol, citric acid, palmitic acid or farnesene from cytosolic acetyl-CoA. Lumped stoichiometries are given by Reactions (20)–(23).
- Introduction of NAD^+-dependent acetaldehyde dehydrogenase, in addition to the $NADP^+$-dependent reaction present in the original model, thereby introducing redox cofactor flexibility in the PDH bypass.
- Introduction of ATP-citrate lyase to enable the citrate-oxaloacetate shuttle.
- Introduction of independent phosphoketolase activities with fructose-6-phosphate and xylulose-5-phosphate as the substrate; introduction of phosphotransacetylase.
- Introduction of NAD^+-dependent acetylating acetaldehyde dehydrogenase. The following three oxidative, ATP-independent options from pyruvate to acetyl-CoA (Table 1) have the same overall stoichiometry as the acetylating acetaldehyde dehydrogenase-based pathway and are therefore not individually modelled: cytosolic PDH complex, pyruvate-formate lyase with formate dehydrogenase and export of mitochondrial acetyl moieties to the cytosol via the carnitine shuttle.
- To facilitate NADH generation via the TCA-cycle for products with a degree of reduction that is higher than that of glucose, the succinate dehydrogenase reaction was modified to use NAD^+ instead of FAD^+. In practice, this could for instance be achieved by overexpressing an NADH-dependent fumarate reductase (Salusjarvi et al., 2013; Yan et al., 2014).

Table 2
Overall stoichiometry for the formation of 1 mole of *n*-butanol with glucose as the sole source of electrons ($C_4H_{10}O$; γ=24 e-mol mol^{-1}). The Gibbs free energy change under biochemical standard conditions ($\Delta G_R^{\circ\prime}$) for the theoretical maximum reaction stoichiometry is estimated at -265.9 ± 12.6 kJ mol^{-1} (Flamholz et al., 2012). Overall reaction stoichiometries are obtained using MetaTool 5.1 (Von Kamp and Schuster, 2006), based on an adapted version of the stoichiometric model of central carbon metabolism of *S. cerevisiae* by Carlson et al. (2002). The listed reaction stoichiometry for each pathway represents the flux solution with the highest product yield on substrate. Any ATP requirement was preferentially met by reoxidation of surplus NADH. If additional ATP was required, additional glucose was used for complete respiratory dissimilation to generate the remaining ATP (P/O ratio assumed to be 1 (Verduyn et al., 1991)). Surplus NADH not required for ATP generation and/or ATP generated from the product formation pathways are indicated in the stoichiometry. For simplicity, the reactants NAD^+, ADP, P_i and H^+ are not shown.

Pathway	Reaction stoichiometry	Yield (mol_p/mol_s)
Theoretical maximum	glucose → *n*-butanol + 2 CO_2 + H_2O	1
PDH bypass	$1\frac{1}{8}$ glucose + $\frac{3}{4}$ O_2 → *n*-butanol + $2\frac{3}{4}$ CO_2 + $1\frac{3}{4}$ H_2O	0.889
Citrate-oxaloacetate shuttle with ACL	glucose → *n*-butanol + 2CO_2 + H_2O	1
Phosphoketolase/-transacetylase	glucose → *n*-butanol + 2CO_2 + H_2O + ATP	1
ATP-independent pyruvate to acetyl-CoA routes[a]	glucose → *n*-butanol + 2CO_2 + H_2O + 2ATP	1

[a] These pathway use either A-ALD, PDH_{cyt}, PDH_{mit} with the carnitine shuttle or, when conditions are anaerobic, PFL with FDH.

cultures (Fendt and Sauer, 2010; Gancedo, 1998).

Comparison of *n*-butanol formation from glucose via the four different pathways for acetyl-CoA formation clearly demonstrates their impact on product yield. The ATP cost of the ACS reaction in the PDH bypass necessitates respiratory dissimilation of glucose, constraining the maximum attainable yield of *n*-butanol to 0.889 mol (mol glucose)$^{-1}$. This pathway configuration therefore precludes anaerobic, fermentative *n*-butanol production (Table 2). Production of *n*-butanol from glucose is ATP neutral when acetyl-CoA is formed via the citrate-oxaloacetate shuttle. This configuration, however, still requires another dissimilatory pathway to provide ATP for growth and cellular maintenance. The remaining two pathways for acetyl-CoA formation enable production of *n*-butanol at the maximum theoretical yield of 1 mol (mol glucose)$^{-1}$ and with a positive ATP yield, thereby potentially allowing for an anaerobic, fermentative process. Use of the PK/PTA route partially bypasses the substrate phosphorylation steps of glycolysis and therefore yields only 1 mole of ATP per mole of *n*-butanol. ATP-independent, oxidative conversion of pyruvate to acetyl-CoA (A-ALD, PDH_{cyt} and PFL/FDH) enables the formation of 2 moles of ATP per mole of *n*-butanol, which is identical to the ATP yield from classical alcoholic fermentation of glucose by *S. cerevisiae*.

3.2. Citric acid

Citric acid, a six-carbon tricarboxylic acid, is currently produced on an industrial scale using *A. niger* and can, alternatively, be produced with the yeast *Y. lipolytica* (Max et al., 2010). Since citric acid is more oxidized than glucose (degrees of reduction 18 and 24, respectively), it represents an interesting model product to theoretically explore how redox-cofactor balancing of precursor supply and product pathways can affect product yield. The key enzyme in citric acid production (Fig. 2B), citrate synthase, uses acetyl-CoA and oxaloacetate as substrates:

$$\text{acetyl-CoA} + \text{oxaloacetate} + H_2O = \text{citrate} + \text{CoA}. \quad (21)$$

In *A. niger*, and likely also in *Y. lipolytica*, citrate synthase is localized in the mitochondrial matrix (Ruijter et al., 2000). However, for this theoretical assessment of the impact of the different cytosolic acetyl-CoA formation pathways on product yield, we will assume a cytosolic localization. Formation of oxaloacetate from glucose via the ATP-dependent carboxylation of pyruvate (EC 6.4.1.1; $\text{pyruvate} + CO_2 + \text{ATP} + H_2O = \text{oxaloacetate} + \text{ADP} + P_i$) results in the formation of 1 NADH. Additionally, all oxidative routes for acetyl-CoA formation result in the formation of an additional 2 NADH per citric acid. This 'excess' NADH can be reoxidized by mitochondrial respiration, thus providing ATP for growth, maintenance, product export and, in some pathway configurations, for acetyl-CoA formation (Table 3). Oxidative formation of acetyl-CoA from pyruvate limits the maximum attainable yield of citric acid to 1 mol (mol glucose)$^{-1}$ (Table 3), which is substantially lower than the theoretical maximum yield of citric acid on glucose (1.33 mol mol^{-1}; Table 3). As described above, conversion of glucose to acetyl-CoA via the PK/PTA pathway does not result in NADH formation and even enables net incorporation of CO_2 into the product. Use of PK/PTA for acetyl-CoA synthesis should therefore enable a higher maximum attainable citrate yield on

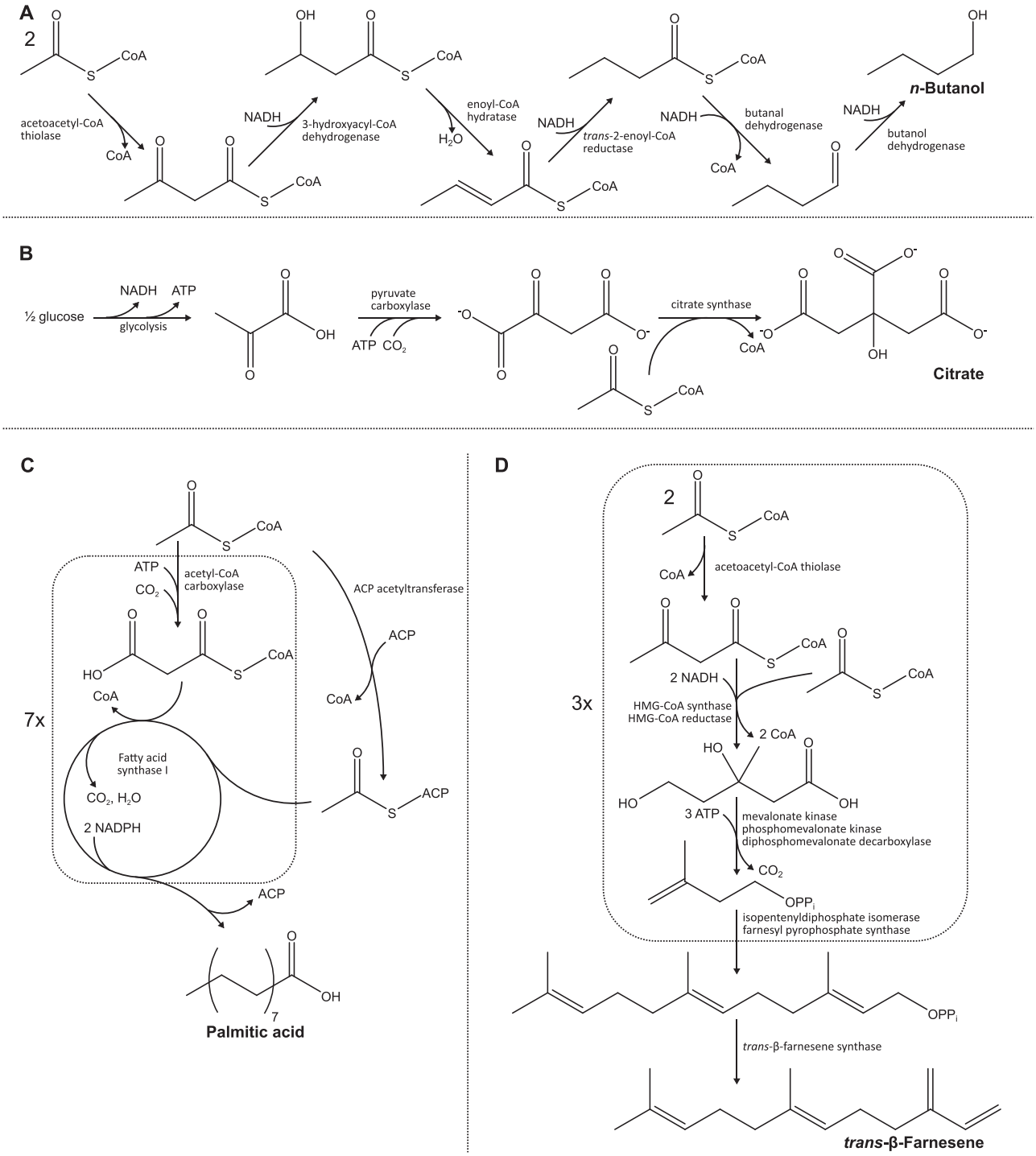

Fig. 2. Pathways for synthesis of four model compounds starting from cytosolic acetyl-CoA as the (main) precursor: A *n*-butanol, B citrate, C palmitic acid and D *trans*-β-farnesene. Pathways are adapted and based on MetaCyc pathways PWY-6883, PWY-5750, PWY-922, PWY-5123 and PWY-5725 (Caspi et al., 2014) and on the review by Tehlivets et al. (2007).

glucose of 1.2 mol mol^{-1} (Table 3), which corresponds to 90% of the maximum theoretical yield (Table 3). Engineering acetyl-CoA formation via the PK/PTA route into *Y. lipolytica* and *A. niger* might therefore be an interesting approach to increase citric acid yield on glucose. Interestingly, both microorganisms already harbor a cytosolic PK and, thereby, only seems to lack a functional PTA (Dujon et al., 2004; Pel et al., 2007; Ratledge and Holdsworth, 1985). This strategy does not only have the potential to increase the citric acid yield on glucose, but also to increase the product yield on oxygen. The lower ATP yield from citric acid formation via a PK/PTA pathway can be beneficial for minimizing growth, although ATP availability will be required for cellular maintenance, especially at the low pH values that are typical for these processes.

3.3. Palmitic acid

Microbial production of lipids, whose applications range from biofuels to cosmetics, is intensively investigated (Rude and Schirmer, 2009; Sheng and Feng, 2015). As a model compound, we consider palmitic acid, a saturated C_{16} fatty acid that is considerably more

Table 3
Overall stoichiometry for the formation of 1 mole of citric acid with glucose as the sole source of electrons ($C_6H_8O_7$; γ=18 e-mol mol^{-1}). The Gibbs free energy change under biochemical standard conditions ($\Delta G_R^{\circ\prime}$) for the theoretical maximum reaction stoichiometry is estimated at -143.5 ± 9.1 kJ mol^{-1} (Flamholz et al., 2012). Overall reaction stoichiometries are obtained using MetaTool 5.1 (Von Kamp and Schuster, 2006), based on an adapted version of the stoichiometric model of central carbon metabolism of *S. cerevisiae* by Carlson et al. (2002). The listed reaction stoichiometry for each pathway represents the flux solution with the highest product yield on substrate. Any ATP requirement was preferentially met by reoxidation of surplus NADH. If additional ATP was required, additional glucose was used for complete respiratory dissimilation to generate the remaining ATP (P/O ratio assumed to be 1 (Verduyn et al., 1991)). Surplus NADH not required for ATP generation and/or ATP generated from the product formation pathways are indicated in the stoichiometry. For simplicity, the reactants NAD^+, ADP, P_i and H^+ are not shown.

Pathway	Reaction stoichiometry	Yield (mol_p/mol_s)
Theoretical maximum	$\frac{3}{4}$ glucose + $1\frac{1}{2}$ CO_2 → citrate + $\frac{1}{2}$ H_2O	1.333
PDH bypass	glucose + $\frac{1}{2}$ O_2 → citrate + 2 NADH	1
Citrate-oxaloacetate shuttle with ACL	N.A.	N.A.
Phosphoketolase/-transacetylase	$\frac{5}{6}$ glucose + CO_2 → citrate + NADH	1.2
ATP-independent pyruvate to acetyl-CoA routes[a]	glucose → citrate + 3 NADH + ATP	1

[a] These pathway use either A-ALD, PDH_{cyt}, PDH_{mit} with the carnitine shuttle or, when conditions are anaerobic, PFL with FDH.

Table 4
Overall stoichiometry for the formation of 1 mole of palmitic acid with glucose as the sole source of electrons ($C_{16}H_{32}O_2$; γ=92 e-mol mol^{-1}). The Gibbs free energy change under biochemical standard conditions ($\Delta G_R^{\circ\prime}$) for the theoretical maximum reaction stoichiometry is estimated at -1161.2 ± 42.2 kJ mol^{-1} (Flamholz et al., 2012). Overall reaction stoichiometries are obtained using MetaTool 5.1 (Von Kamp and Schuster, 2006), based on an adapted version of the stoichiometric model of central carbon metabolism of *S. cerevisiae* by Carlson et al. (2002). The listed reaction stoichiometry for each pathway represents the flux solution with the highest product yield on substrate. Any ATP requirement was preferentially met by reoxidation of surplus NADH. If additional ATP was required, additional glucose was used for complete respiratory dissimilation to generate the remaining ATP (P/O ratio assumed to be 1 (Verduyn et al., 1991)). Surplus NADH not required for ATP generation and/or ATP generated from the product formation pathways are indicated in the stoichiometry. For simplicity, the reactants NAD^+, ADP, P_i and H^+ are not shown.

Pathway for acetyl-CoA formation	Stoichiometry for formation of 1 palmitic acid	Yield (mol_p/mol_s)
Theoretical maximum	$3\frac{5}{6}$ glucose → palmitic acid + 7CO_2 + 7H_2O	0.261
PDH bypass	$4\frac{11}{12}$ glucose + $6\frac{1}{2}$ O_2 → palmitic acid + $13\frac{1}{2}$ CO_2 + $13\frac{1}{2}$ H_2O	0.203
Citrate-oxaloacetate shuttle with ACL	$5\frac{1}{6}$ glucose + $3\frac{1}{2}$ O_2 → palmitic acid + 15 CO_2 + 6 H_2O + 9NADH	0.194
Phosphoketolase/-transacetylase	$4\frac{3}{7}$ glucose + $3\frac{4}{7}$ O_2 → palmitic acid + $10\frac{4}{7}$ CO_2 + $10\frac{4}{7}$ H_2O	0.226
ATP-independent pyruvate to acetyl-CoA routes[a]	$5\frac{1}{6}$ glucose → palmitic acid + 15CO_2 + 16NADH + ATP	0.194
Optimal combinatorial configuration[b]	$4\frac{3}{10}$glucose + $2\frac{8}{10}$ O_2 → palmitic acid + $9\frac{4}{5}$ CO_2 + $9\frac{4}{5}$$H_2O$	0.232

[a] These pathway use either A-ALD, PDHcyt, PDHmit with the carnitine shuttle or, when conditions are anaerobic, PFL with FDH.
[b] 65% via phosphoketolase/-transacetylase and 35% via an ATP-independent pyruvate to acetyl-CoA route.

reduced than glucose ($5\frac{3}{4}$ e-mol C-mol^{-1} and 4 e-mol C-mol^{-1}, respectively). Its theoretical maximum yield on glucose is 0.261 mol mol^{-1}. In the yeast cytosol, palmitic acid is synthesized by a type-I fatty acid synthase (Tehlivets et al., 2007). Synthesis of palmitic acid starts with an acetyl moiety, originating from cytosolic acetyl-CoA, as a primer. The following 7 cycles of elongation use malonyl-CoA, which is also produced from cytosolic acetyl-CoA, as acetyl donor and involve the use of 2 NADPH for each elongation step (Fig. 2C). When synthesis of malonyl-CoA from cytosolic acetyl-CoA by acetyl-CoA carboxylase (EC 6.4.1.2), which requires 1 ATP per malonyl-CoA, is included, the net reaction for formation of palmitic acid from acetyl-CoA (Fig. 2C) is:

$$8\text{acetyl-CoA} + 7\text{ATP} + 14(\text{NADPH} + \text{H}^+) + \text{H}_2\text{O} = \text{palmitic acid} + 8\text{CoA} + 14\text{NADP}^+ + 7(\text{ADP} + \text{P}_i). \quad (22)$$

Stoichiometric analysis reveals the impact of redox-cofactor balancing on the palmitic-acid yield on glucose (Table 4). NADPH is the preferred electron donor in fatty acid synthesis pathways, while NADH is formed in most pathways that convert glucose into acetyl-CoA (Table 4). Combining these precursor supply and product pathways therefore not only requires a large additional flux through the oxidative pentose-phosphate pathway to generate NADPH, but also generates a large amount of NADH. When palmitic acid production uses cytosolic acetyl-CoA generated by the NAD^+-dependent PDH bypass route, all NADH generated in precursor supply has to be reoxidized to NAD^+ to provide ATP required for the ACS reaction. Use of the citrate-oxaloacetate shuttle, which has a lower ATP requirement for acetyl-CoA synthesis, leaves a larger fraction of the NADH from palmitic acid production unused (Table 4). This fraction increases even further when any of the ATP-independent pathways towards cytosolic acetyl-CoA are used (Table 4). Respiratory reoxidation of this 'excess' NADH respiration generates ATP, which enables extensive diversion of glucose to biomass formation, thereby decreasing product yields. As a result of this imbalance between NADH production and NADPH consumption, the citrate-oxaloacetate shuttle and the ATP-independent acetyl-CoA formation routes result in the lowest attainable palmitic acid yields (0.194 mol mol^{-1}; Table 4).

The two remaining pathways for cytosolic acetyl-CoA formation are intrinsically more flexible in balancing NADH and NADPH generation with cellular requirements. In the PDH bypass, involvement of $NADP^+$-dependent acetaldehyde dehydrogenase can provide part of the NADPH required in Reaction (22), whilst simultaneously decreasing the formation of excess NADH. In contrast to the other pathways for cytosolic acetyl-CoA production from glucose, the PK/PTA pathway does not result in NADH formation (Fig. 1B). This property is highly advantageous for palmitic acid production and enables a maximum attainable yield of palmitic acid to glucose that corresponds to 87% of the maximum theoretical yield when NADPH formation occurs via the oxidative pentose-phosphate pathway (Table 4). An even higher maximum attainable yield can be obtained by combining the PK/PTA pathway with an ATP-independent route from pyruvate to acetyl-CoA. In an optimal scenario, 65% of the acetyl-CoA should then be derived from the PK/PTA pathway, enabling a maximum attainable yield that corresponds to 89% of the theoretical maximum.

Regardless of the acetyl-CoA synthesis route, the dependence of the discussed pathways on respiration to produce ATP and/or to regenerate NAD^+ precludes the synthesis of palmitic acid a sole catabolic pathway under anaerobic conditions. Interestingly, some organisms do rely on fatty-acid synthesis as a catabolic, ATP generating pathway. For example, *Euglena gracilis* ferments sugars, via fatty acids, to wax esters, which can constitute up to 60% of its dry mass (Tucci et al., 2010). In this organism, pyruvate is converted to acetyl-CoA via the chimeric PFO/PFR system discussed above (Inui et al., 1991, 1984a). Moreover, fatty acid synthesis in *E. gracilis* does

not rely on a malonyl-CoA-dependent fatty acid synthase pathway, but on a reversed β-oxidation pathway, which does not involve ATP hydrolysis (Khan and Kolattukudy, 1973).

3.4. Farnesene

The sesquiterpene *trans*-β-farnesene is a C_{15} branched, unsaturated hydrocarbon, which can be used for production of diesel fuel, polymers and cosmetics (Rude and Schirmer, 2009). Farnesene can be produced from 3 molecules of mevalonate, generated in the eukaryotic isoprenoid biosynthesis pathway. The mevalonate pathway not only requires large amounts of ATP (see Reaction (23)), but also combines all previously mentioned challenges in balancing NADH, NADPH and ATP conversions. *S. cerevisiae*, which does not naturally synthesize *trans*-β-farnesene, has been genetically modified to produce this compound at high titers and yields (Sandoval et al., 2014). One of the mevalonate pathway enzymes, HMG-CoA reductase, uses NADPH. To reduce the need for extensive glucose oxidation via the oxidative pentose phosphate pathway, this enzyme has been successfully replaced by an NADH-dependent HMG-CoA reductase (Gardner et al., 2013), thus enabling the following reaction stoichiometry for formation of farnesene from acetyl-CoA (Fig. 2D):

$$9\text{acetyl-CoA} + 6(\text{NADH} + \text{H}^+) + 9\text{ATP} + 6\text{H}_2\text{O} = \text{farnesene} + 9\text{CoA} + 6\,\text{NAD}^+ + 9\,(\text{ADP} + \text{P}_i) + 3\text{CO}_2 \quad (23)$$

The maximum theoretical yield of farnesene on glucose is 0.286 mol mol^{-1} (Table 5). When using the native PDH bypass for cytosolic acetyl-CoA formation, the high ATP cost for acetyl-CoA synthesis via ACS necessitates respiratory dissimilation of over one mole of glucose per mole of farnesene. This ATP requirement limits the maximum attainable yield of farnesene on glucose to only 0.205 mol mol^{-1}. The more ATP-efficient routes for acetyl-CoA synthesis via the citrate-oxaloacetate shuttle and the ATP-independent routes from pyruvate to acetyl-CoA enable significantly higher maximum attainable yields of 0.222 mol (mol glucose)$^{-1}$. In both routes, 18 NADH is formed per 9 acetyl-CoA, while only 6 NADH is consumed in the synthesis of farnesene from acetyl-CoA (Reaction (23)). When using the citrate-oxaloacetate shuttle, 9 of the remaining 12 NADH need to be oxidized to provide ATP for farnesene synthesis. In the absence of other catabolic pathways, this would only leave 3 NADH to provide ATP for growth and cellular maintenance via oxidative phosphorylation. Conversely, when ATP-independent routes for acetyl-CoA synthesis are used, all 12 moles NADH generated per mole of farnesene are available for ATP production to sustain growth and maintenance.

The absence of NADH generation makes the PK/PTA pathway the most attractive of the four individual routes, with a maximum attainable yield of 0.246 mol (mol glucose)$^{-1}$, which corresponds 86% of the maximum theoretical yield. The deviation of this maximum attainable yield from the theoretical yield is caused by the need for respiratory dissimilation of part of the glucose to provide the required ATP. In theory, the maximum attainable yield of farnesene on glucose can be further improved by combining the PK/PTA pathway with any of the ATP-independent pyruvate-to-acetyl-CoA pathways, resulting in a maximum attainable yield of farnesene on glucose of up to 91% of the theoretical maximum. This requires a pathway configuration in which, for each mole of farnesene, 4 moles of acetyl-CoA are produced via the PK/PTA pathway and 5 moles of acetyl-CoA via an ATP-independent route from pyruvate to acetyl-CoA. In this scenario, oxygen is still required to provide ATP, but this requirement is reduced to 2 mole of oxygen per mole of farnesene. In industrial practice, additional oxygen may, however, be required to provide ATP for growth and cellular maintenance.

4. Kinetics and thermodynamics

Stoichiometric analysis of metabolic pathways provides valuable insights to shape metabolic engineering strategies. However, implementation of a (heterologous) route in an industrial strain not only demands high product yields, but also high productivities. Therefore, not only the stoichiometry, but also the thermodynamic driving force (ΔG_R), the ensuing intracellular concentrations of metabolites and the enzyme kinetics of the enzymes (V_{max}, K_M) have to be considered. Below, we briefly discuss observations on engineering of cytosolic acetyl-CoA synthesis that affect the delicate balance between kinetics and stoichiometry.

The biosynthetic and regulatory requirements for acetyl-CoA in the cytosol and nucleus of wild-type *S. cerevisiae* require only relatively low fluxes through the PDH bypass (Kozak et al., 2014a). Shiba et al. (2007) engineered the native *S. cerevisiae* PDH bypass pathway (Fig. 1A) for cytosolic acetyl-CoA synthesis by overexpression of the responsible enzymes (Shiba et al., 2007). ALD and ACS activities were increased by overexpressing the native cytosolic NADP$^+$-dependent acetaldehyde dehydrogenase Ald6 and a heterologous ACS from *Salmonella enterica*, respectively. Since high intracellular acetyl-CoA levels can inhibit ACS enzymes by acetylation of a lysine residue, the *S. enterica* ACS was

Table 5
Overall stoichiometry for the formation of 1 mole of *trans*-β-farnesene with glucose as the sole source of electrons ($C_{15}H_{24}$; γ=84 e-mol mol^{-1}). The Gibbs free energy change under biochemical standard conditions ($\Delta G_R^{\circ\prime}$) for the theoretical maximum reaction stoichiometry is estimated at -870.1 ± 39.3 kJ mol^{-1} (Flamholz et al., 2012). Overall reaction stoichiometries are obtained using MetaTool 5.1 (Von Kamp and Schuster, 2006), based on an adapted version of the stoichiometric model of central carbon metabolism of *S. cerevisiae* by Carlson et al. (2002). The listed reaction stoichiometry for each pathway represents the flux solution with the highest product yield on substrate. Any ATP requirement was preferentially met by reoxidation of surplus NADH. If additional ATP was required, additional glucose was used for complete respiratory dissimilation to generate the remaining ATP (P/O ratio assumed to be 1 (Verduyn et al., 1991)). Surplus NADH not required for ATP generation and/or ATP generated from the product formation pathways are indicated in the stoichiometry. For simplicity, the reactants NAD$^+$, ADP, P_i and H$^+$ are not shown.

Pathway	Reaction stoichiometry	Yield (mol_p/mol_s)
Theoretical maximum	$3\frac{1}{2}$ glucose → farnesene + 6 CO_2 + 9H_2O	0.286
PDH bypass	$4\frac{7}{8}$glucose + $8\frac{1}{4}$ O_2 → farnesene + $14\frac{1}{4}$ CO_2 + $17\frac{1}{4}H_2O$	0.205
Citrate-oxaloacetate shuttle with ACL	$4\frac{1}{2}$ glucose + $4\frac{1}{2}$ O_2 → farnesene + 12CO_2 + 12H_2O + 3NADH	0.222
Phosphoketolase/-transacetylase	$4\frac{1}{17}$glucose + $3\frac{6}{17}$ O_2 → farnesene + $9\frac{6}{17}$ CO_2 + $12\frac{6}{17}H_2O$	0.246
ATP-independent pyruvate to acetyl-CoA routes[a]	$4\frac{1}{2}$ glucose → farnesene + 12CO_2 + 3H_2O + 12NADH	0.222
Combinatorial configuration[b]	$3\frac{5}{6}$glucose + 2O_2 → farnesene + 8CO_2 + 11H_2O	0.261

[a] These pathway use either A-ALD, PDHcyt, PDHmit with the carnitine shuttle or, when conditions are anaerobic, PFL with FDH.
[b] 44% via phosphoketolase/-transacetylase and 56% via an ATP-independent pyruvate to acetyl-CoA route.

engineered to prevent acetylation through an L641P amino acid substitution. These modifications substantially increased *in vitro* ALD and ACS activities and, importantly, improved the *in vivo* synthesis rate of amorphadiene, a product derived from cytosolic acetyl-CoA via the mevalonate pathway, by 1.8 fold. This result shows that the PDH bypass can be engineered to sustain higher *in vivo* fluxes towards industrially relevant compounds.

While alternative acetyl-CoA-forming pathways are stoichiometrically superior to the PDH bypass, their expression in *S. cerevisiae* has revealed some interesting challenges related to *in vivo* kinetics. As discussed above, the PFL pathway theoretically enables ATP-efficient production of acetyl-CoA under anaerobic conditions. Additionally, the turnover number of PFL enzymes is generally high $\sim 10^3\ s^{-1}$ (Knappe et al., 1974). However, efficient use of this pathway requires that formic acid, which is co-produced with acetyl-CoA, is re-oxidized to CO_2 by NAD^+-dependent formate dehydrogenase (FDH). Achieving high *in vivo* FDH activities in *S. cerevisiae* is a highly non-trivial challenge because of the low turnover numbers ($\sim 10\ s^{-1}$) of currently characterized NAD^+-dependent FDH enzymes (Chang et al., 2014). In chemostat cultures of an *S. cerevisiae* Acs^- strain expressing *E. coli* PFL (Kozak et al., 2014a), accumulation of formate showed that native FDH activity was insufficient to oxidize excess formate. Previous attempts to increase *in vivo* FDH activity in anaerobic cultures of *S. cerevisiae* by overexpression of its *FDH1* gene were not only complicated by the low turnover number of its gene product, but also by the negative impact of high $NADH/NAD^+$ ratios on its enzyme activity (Geertman et al., 2006). Increasing the *in vivo* capacity and activity of FDH is therefore a priority target for successful implementation of the PFL pathway for acetyl-CoA synthesis in *S. cerevisiae*.

In a recent study, co-expression of the *Clostridium n*-butanol pathway with four different cytosolic acetyl-CoA forming pathways in *S. cerevisiae* resulted in only small increases of an already low butanol yield (Lian et al., 2014). These studies indicate that optimization of the flux through these heterologous acetyl-CoA and product-forming pathways is often required. Ideally, experiments for assessing the kinetics of alternative precursor supply pathways should be performed in strain backgrounds with a high overcapacity of all reactions downstream of the precursor.

Compatibility of a heterologous enzyme with a metabolic engineering strategy may not only be determined by its *in vivo* capacity (V_{max}) in the host organism, but also by its affinity ($\frac{V_{max}}{K_M}$), which dictates the intracellular concentration of its substrate that is required to achieve a target flux. Affinity is especially important when the substrate of an enzyme is toxic, as is the case for A-ALD (Reaction (8)), which shows a much lower affinity for acetaldehyde than the native yeast acetaldehyde dehydrogenase isoenzymes (Kozak et al., 2014a). Consistent with this observation, yeast strains in which the native yeast ALDs were replaced by heterologous A-ALDs showed elevated intracellular acetaldehyde levels. Acetaldehyde toxicity was implicated in the lower than expected biomass yields of these engineered strains.

The elevated acetaldehyde concentrations in A-ALD dependent strains may not solely reflect a kinetic requirement. Although, as mentioned above, $\Delta G_R^{\circ\prime}$ of the A-ALD reaction (Reaction (8)) is negative, biochemical standard conditions are unlikely to reflect the thermodynamics of this reaction in the yeast cytosol. Assuming an $[NADH]/[NAD^+]$ ratio of 0.01 (Canelas et al., 2008), the $\Delta G_R'$ of the reaction at the acetaldehyde levels that were measured in wild-type *S. cerevisiae* was estimated to be $+7.2\ kJ\ mol^{-1}$ (Kozak et al., 2014a), which would render use of the A-ALD pathway for acetyl-CoA synthesis thermodynamically impossible. The observed increased acetaldehyde concentrations in an A-ALD-dependent strain increased the estimated $\Delta G_R'$ of the reaction close to zero ($+0.7\ kJ\ mol^{-1}$) (Kozak et al., 2014a). This observation suggests that toxic levels of acetaldehyde may have been a thermodynamic prerequisite to allow the A-ALD reaction to proceed in the oxidative reactions in the yeast cytosol.

As described above, in their metabolic engineering strategy for farnesene production, Gardner et al. (2013) replaced the native *S. cerevisiae* HMG-CoA reductase, which is NADPH dependent, for an NADH-dependent enzyme. Interestingly, strains with an NADH-dependent HMG-CoA reductase exhibited approximately 4-fold lower intracellular mevalonate levels than strains expressing the NADPH-dependent enzyme (Gardner et al., 2013). The $[NADPH]/[NADP^+]$ ratio in the yeast cytosol is generally much higher than the $[NADH]/[NAD^+]$ (under aerobic conditions: 15.6–22.0 as compared to 0.01, respectively; Canelas et al., 2008; Zhang et al., 2015a). When these different 'redox charges' of the two cofactor couples are taken into account, the thermodynamic driving force for the NADH-dependent reaction is much less favorable (difference in $\Delta G_R'$ $\sim 40\ kJ\ mol^{-1}$) than for the NADPH-dependent reaction. This difference in $\Delta G_R'$ offers a plausible explanation for the kinetically superior performance of the NADPH-dependent native HMG-CoA reductase. Consistent with this interpretation, deletion of the gene encoding the Adh2 alcohol dehydrogenase, which was anticipated to lead to higher cytosolic $[NADH]/[NAD^+]$ ratios, indeed led to increased mevalonate levels (Gardner et al., 2013). These examples illustrate how not only stoichiometry, but also kinetics and thermodynamics need to be considered when designing metabolic engineering strategies to optimize acetyl-CoA provision.

5. Discussion and outlook

This review focused on reaction stoichiometry, kinetics and thermodynamics of alternative pathways for providing acetyl-CoA, a key precursor for the formation of many industrially relevant compounds, in the yeast cytosol. Several of the acetyl-CoA- producing pathways discussed here have recently been successfully expressed in *S. cerevisiae*, thereby providing metabolic engineers with new options to optimally align and integrate precursor supply with product pathways downstream of acetyl-CoA (Nielsen, 2014). The stoichiometric analyses discussed above show how the optimal pathway configuration for the synthesis of a single metabolic precursor, cytosolic acetyl-CoA, is strongly product dependent. This observation underlines the importance of evaluating multiple pathways for precursor supply at the outset of metabolic engineering projects.

In general terms, the PK/PTA provides the highest possible carbon conversion of the routes discussed in this paper, while the acetyl-CoA forming routes via A-ALD, PDH or PFL/FDH enable the net formation of ATP. In addition to ATP formation, cofactor balancing is another key factor in defining the optimal precursor supply strategy. Stoichiometric evaluation of individual acetyl-CoA forming routes for a given product pathway already provide valuable leads for improving product yield on substrate. However, as illustrated by the examples of palmitic acid production and farnesene production (Tables 4 and 5), combinations of different precursor supply routes can lead to even higher maximum product yields. To achieve the stoichiometric potential of combined routes requires that the relative *in vivo* activities of the contributing precursor supply pathways can be accurately controlled, even under dynamic industrial conditions. Achieving such accurately tunable *in vivo* flux distributions and, consequently, optimal product yields, represents a highly relevant challenge for metabolic engineers.

In this review, we limited our discussion of cytosolic acetyl-CoA supply in yeast to pathways that naturally occur in heterotrophic

organisms. Implementation of autotrophic acetyl-CoA forming pathways in *S. cerevisiae* provides additional highly interesting scientific challenges and possibilities. For example, the Wood-Ljungdahl pathway, or reductive acetyl-CoA pathway, is used by acetogens to conserve free energy and to generate acetyl-CoA for growth (Ljungdahl and Wood, 1969). In an otherwise heterotrophic cell factory, this system could be useful to donate excess electrons to CO_2 for the synthesis of additional acetyl-CoA, according to the overall stoichiometry:

$$2CO_2 + 8(e^- + H^+) + ATP + CoA = \text{acetyl-CoA} + 2H_2O + ADP + P_i. \quad (24)$$

Functional expression of the enzymes of this system in *S. cerevisiae* itself already present a formidable challenge, while complexity is further increased by the use of different redox cofactors: H_2, reduced ferredoxin and/or NAD(P)H (Schuchmann and Müller, 2014). Several other autotrophs use a reductive TCA cycle to produce acetyl-CoA from CO_2, with the following overall reaction stoichiometry (Buchanan and Arnon, 1990):

$$2CO_2 + 8\,(e^- + H^+) + 2\ ATP + CoA = \text{acetyl-CoA} + H_2O + 2\,(ADP + P_i) \quad (25)$$

An important difference with the conventional oxidative TCA cycle is the involvement of an α-ketoglutarate ferredoxin oxidoreductase (EC 1.2.7.3), which enables the *in vivo* carboxylation of succinyl-CoA to α-ketoglutarate, and of ATP-citrate lyase (ACL), which cleaves citrate into oxaloacetate and acetyl-CoA. Although the ATP stoichiometry of this pathway is less favourable than that of the Wood-Ljungdahl pathway, two aspects might make it (slightly) less challenging to functionally express this system in *S. cerevisiae*. Firstly, while reduced ferredoxin as an electron donor is required for the α-ketoglutarate dehydrogenase reaction, the remaining redox reactions in the reductive TCA cycle use NADH as cofactor. Secondly, the enzymes involved in the reductive TCA cycle are generally less complex and some, such as ACL, have already been successfully expressed in yeast (see above).

Producing industrially relevant compounds of interest at near-theoretical yields requires that, if thermodynamically possible, all electrons from the substrate end up in the product. Instead, in many of the scenarios analyzed in this review, precursor formation resulted in formation of excess NADH (Tables 2–5). In other cases, NADH was required to enable ATP formation via oxidative phosphorylation, to provide the free-energy for product formation and cellular maintenance. Only in the case of *n*-butanol formation via the A-ALD, PDH or PFL/FDH pathway, a redox-neutral, ATP-yielding pathway could be assembled, which should theoretically allow for the maximum theoretical yield in non-growing cultures. For the pathway combinations that yielded excess ATP and/or NADH, implementation of autotrophic acetyl-CoA yielding pathways, or alternatively the expression of the Calvin-cycle enzymes phosphoribulokinase and RuBisCO (Guadalupe-Medina et al., 2013), might further increase the yields of the products of interest. Another recent development that may ultimately contribute to the production of fatty acids as catabolic, anaerobic products in *S. cerevisiae*, is the recent expression of a reverse β-oxidation cycle in the yeast cytosol (Lian and Zhao, 2015b). This pathway for fatty acid synthesis is ATP-independent and, instead of NADPH, has NADH as the redox cofactor. Combining this system with the PK/PTA pathway and an ATP-independent route from pyruvate to acetyl-CoA can, at least theoretically, result in a redox-neutral and ATP yielding pathway.

In addition to quantitative insight into pathway stoichiometry, knowledge about the thermodynamics and kinetics of individual reactions and about the biochemical context in which the corresponding enzymes have to operate, is of crucial importance for evaluating alternative metabolic engineering strategies and to find targets for further optimization. Powerful algorithms for metabolic network evaluation that include thermodynamic and kinetic analyses are among the valuable new tools to find engineering targets and rank alternative strategies (Chakrabarti et al., 2013; Henry et al., 2007; Sánchez and Nielsen, 2015; Soh et al., 2012).

Acknowledgement

This work was carried out within the BE-Basic R&D Program, which was granted an FES subsidy from the Dutch Ministry of Economic Affairs, Agriculture and Innovation (EL&I) and received additional financial contributions from DSM Biotechnology Center and Amyris Inc. Liang Wu (DSM) and Kirsten Benjamin (Amyris) are gratefully acknowledged for a fruitful collaboration and many constructive discussions.

Appendix A. Supplementary material

Supplementary data associated with this article can be found in the online version at http://dx.doi.org/10.1016/j.ymben.2016.03.006.

References

Aouida, M., Rubio-Texeira, M., Rubio Texeira, M., Thevelein, J.M., Poulin, R., Ramotar, D., 2013. Agp2, a member of the yeast amino acid permease family, positively regulates polyamine transport at the transcriptional level. PLoS One 8, e65717.
Avalos, J.L., Fink, G.R., Stephanopoulos, G., 2013. Compartmentalization of metabolic pathways in yeast mitochondria improves the production of branched-chain alcohols. Nat. Biotechnol. 31, 335–341.
Bakker, B.M., Overkamp, K.M., Van Maris, A.J.A., Kötter, P., Luttik, M.A.H., Van Dijken, J.P., Pronk, J.T., 2001. Stoichiometry and compartmentation of NADH metabolism in *Saccharomyces cerevisiae*. FEMS Microbiol. Rev. 25, 15–37.
Beekwilder, J., Van Rossum, H.M., Koopman, F., Sonntag, F., Buchhaupt, M., Schrader, J., Hall, R.D., Bosch, D., Pronk, J.T., Van Maris, A.J.A., Daran, J.-M., 2014. Polycistronic expression of a β-carotene biosynthetic pathway in *Saccharomyces cerevisiae* coupled to β-ionone production. J. Biotechnol. 192, 383–392.
Bekers, K.M., Heijnen, J.J., Van Gulik, W.M., 2015. Determination of the *in vivo* NAD: NADH ratio in *Saccharomyces cerevisiae* under anaerobic conditions, using alcohol dehydrogenase as sensor reaction. Yeast 32, 541–557.
Bieber, L.L., 1988. Carnitine. Annu. Rev. Biochem. 57, 261–283.
Bogorad, I.W., Lin, T.-S., Liao, J.C., 2013. Synthetic non-oxidative glycolysis enables complete carbon conservation. Nature 502, 693–697.
Boulton, C.A., Ratledge, C., 1981. Correlation of lipid accumulation in yeasts with possession of ATP:citrate lyase. Microbiology 127, 169–176.
Branduardi, P., Longo, V., Berterame, N.M., Rossi, G., Porro, D., 2013. A novel pathway to produce butanol and isobutanol in *Saccharomyces cerevisiae*. Biotechnol. Biofuels 6, 68.
Brunengraber, H., Lowenstein, J.M., 1973. Effect of (–)-hydroxycitrate on ethanol metabolism. FEBS Lett. 36, 130–132.
Buchanan, B.B., Arnon, D.I., 1990. A reverse KREBS cycle in photosynthesis: consensus at last. Photosynth. Res. 24, 47–53.
Buu, L.-M., Chen, Y.-C., Lee, F.-J.S., 2003. Functional characterization and localization of acetyl-CoA hydrolase, Ach1p, in *Saccharomyces cerevisiae*. J. Biol. Chem. 278, 17203–17209.
Canelas, A.B., Van Gulik, W.M., Heijnen, J.J., 2008. Determination of the cytosolic free NAD/NADH ratio in *Saccharomyces cerevisiae* under steady-state and highly dynamic conditions. Biotechnol. Bioeng. 100, 734–743.
Carlson, R., Fell, D., Srienc, F., 2002. Metabolic pathway analysis of a recombinant yeast for rational strain development. Biotechnol. Bioeng. 79, 121–134.
Caspi, R., Altman, T., Billington, R., Dreher, K., Foerster, H., Fulcher, C.A., Holland, T. A., Keseler, I.M., Kothari, A., Kubo, A., Krummenacker, M., Latendresse, M., Mueller, L.A., Ong, Q., Paley, S., Subhraveti, P., Weaver, D.S., Weerasinghe, D., Zhang, P., Karp, P.D., 2014. The MetaCyc database of metabolic pathways and enzymes and the BioCyc collection of Pathway/Genome Databases. Nucleic Acids Res. 42, D459–D471.
Castegna, A., Scarcia, P., Agrimi, G., Palmieri, L., Rottensteiner, H., Spera, I., Germinario, L., Palmieri, F., 2010. Identification and functional characterization of a novel mitochondrial carrier for citrate and oxoglutarate in *Saccharomyces cerevisiae*. J. Biol. Chem. 285, 17359–17370.
Chakrabarti, A., Miskovic, L., Soh, K.C., Hatzimanikatis, V., 2013. Towards kinetic modeling of genome-scale metabolic networks without sacrificing stoichiometric, thermodynamic and physiological constraints. Biotechnol. J. 8, 1043–1057.
Chang, A., Schomburg, I., Placzek, S., Jeske, L., Ulbrich, M., Xiao, M., Sensen, C.W.,

Schomburg, D., 2014. BRENDA in 2015: exciting developments in its 25th year of existence. Nucleic Acids Res. 43, D439–D446.
Chantrenne, H., Lipmann, F., 1950. Coenzyme A dependence and acetyl donor function of the pyruvate-formate exchange system. J. Biol. Chem. 187, 757–767.
Chen, Y., Zhang, Y., Siewers, V., Nielsen, J., 2015. Ach1 is involved in shuttling mitochondrial acetyl units for cytosolic C2 provision in *Saccharomyces cerevisiae* lacking pyruvate decarboxylase. FEMS Yeast Res. 15, fov015
Choi, J.W., Da Silva, N.A., 2014. Improving polyketide and fatty acid synthesis by engineering of the yeast acetyl-CoA carboxylase. J. Biotechnol. 187, 56–59.
Cronan, J.E., Zhao, X., Jiang, Y., 2005. Function, attachment and synthesis of lipoic acid in *Escherichia coli*. Adv. Microb. Physiol. 50, 103–146.
Cueto-Rojas, H.F., Van Maris, A.J.A., Wahl, S.A., Heijnen, J.J., 2015. Thermodynamics-based design of microbial cell factories for anaerobic product formation. Trends Biotechnol. 33, 534–546.
Dandekar, T., Schuster, S., Snel, B., Huynen, M., Bork, P., 1999. Pathway alignment: application to the comparative analysis of glycolytic enzymes. Biochem. J. 343 (Pt 1), 115–124.
De Jong, B.W., Shi, S., Siewers, V., Nielsen, J., 2014. Improved production of fatty acid ethyl esters in *Saccharomyces cerevisiae* through up-regulation of the ethanol degradation pathway and expression of the heterologous phosphoketolase pathway. Microb. Cell. Fact. 13, 39.
De Kok, S., Kozak, B.U., Pronk, J.T., Van Maris, A.J.A., 2012. Energy coupling in *Saccharomyces cerevisiae*: selected opportunities for metabolic engineering. FEMS Yeast Res. 12, 387–397.
DeLoache, W.C., Russ, Z.N., Narcross, L., Gonzales, A.M., Martin, V.J.J., Dueber, J.E., 2015. An enzyme-coupled biosensor enables (*S*)-reticuline production in yeast from glucose. Nat. Chem. Biol. 11, 465–471.
Dujon, B., Sherman, D., Fischer, G., Durrens, P., Casaregola, S., Lafontaine, I., De Montigny, J., Marck, C., Neuvéglise, C., Talla, E., Goffard, N., Frangeul, L., Aigle, M., Anthouard, V., Babour, A., Barbe, V., Barnay, S., Blanchin, S., Beckerich, J.-M., Beyne, E., Bleykasten, C., Boisramé, A., Boyer, J., Cattolico, L., Confanioleri, F., De Daruvar, A., Despons, L., Fabre, E., Fairhead, C., Ferry-Dumazet, H., Groppi, A., Hantraye, F., Hennequin, C., Jauniaux, N., Joyet, P., Kachouri, R., Kerrest, A., Koszul, R., Lemaire, M., Lesur, I., Ma, L., Muller, H., Nicaud, J.-M., Nikolski, M., Oztas, S., Ozier-Kalogeropoulos, O., Pellenz, S., Potier, S., Richard, G.-F., Straub, M.-L., Suleau, A., Swennen, D., Tekaia, F., Wésolowski-Louvel, M., Westhof, E., Wirth, B., Zeniou-Meyer, M., Zivanovic, I., Bolotin-Fukuhara, M., Thierry, A., Bouchier, C., Caudron, B., Scarpelli, C., Gaillardin, C., Weissenbach, J., Wincker, P., Souciet, J.-L., 2004. Genome evolution in yeasts. Nature 430, 35–44.
Elgersma, Y., Van Roermund, C.W., Wanders, R.J., Tabak, H.F., 1995. Peroxisomal and mitochondrial carnitine acetyltransferases of *Saccharomyces cerevisiae* are encoded by a single gene. EMBO J. 14, 3472–3479.
Evans, C.T., Ratledge, C., 1984. Induction of xylulose-5-phosphate phosphoketolase in a variety of yeasts grown on D-xylose: the key to efficient xylose metabolism. Arch. Microbiol., 48–52.
Farhi, M., Marhevka, E., Masci, T., Marcos, E., Eyal, Y., Ovadis, M., Abeliovich, H., Vainstein, A., 2011. Harnessing yeast subcellular compartments for the production of plant terpenoids. Metab. Eng. 13, 474–481.
Fatland, B.L., Ke, J., Anderson, M.D., Mentzen, W.I., Cui, L.W., Allred, C.C., Johnston, J. L., Nikolau, B.J., Wurtele, E.S., 2002. Molecular characterization of a heteromeric ATP-citrate lyase that generates cytosolic acetyl-coenzyme A in *Arabidopsis*. Plant Physiol. 130, 740–756.
Fendt, S.-M., Sauer, U., 2010. Transcriptional regulation of respiration in yeast metabolizing differently repressive carbon substrates. BMC Syst. Biol. 4, 12.
Flamholz, A., Noor, E., Bar-Even, A., Milo, R., 2012. eQuilibrator – the biochemical thermodynamics calculator. Nucleic Acids Res. 40, 770–775.
Fleck, C.B., Brock, M., 2009. Re-characterisation of *Saccharomyces cerevisiae* Ach1p: fungal CoA-transferases are involved in acetic acid detoxification. Fungal Genet. Biol. 46, 473–485.
Flikweert, M.T., De Swaaf, M., Van Dijken, J.P., Pronk, J.T., 1999. Growth requirements of pyruvate-decarboxylase-negative *Saccharomyces cerevisiae*. FEMS Microbiol. Lett. 174, 73–79.
Franken, J., Kroppenstedt, S., Swiegers, J.H., Bauer, F.F., 2008. Carnitine and carnitine acetyltransferases in the yeast *Saccharomyces cerevisiae*: a role for carnitine in stress protection. Curr. Genet. 53, 347–360.
Gailiusis, J., Rinne, R.W., Benedict, C.R., 1964. Pyruvate-oxaloacetate exchange reaction in Baker's yeast. Biochim. Biophys. Acta 92, 595–601.
Galdieri, L., Zhang, T., Rogerson, D., Lleshi, R., Vancura, A., 2014. Protein acetylation and acetyl coenzyme A metabolism in budding yeast. Eukaryot. Cell. 13, 1472–1483.
Gancedo, C., 1971. Inactivation of fructose-1,6-diphosphatase by glucose in yeast. J. Bacteriol. 107, 401–405.
Gancedo, J.M., 1998. Yeast carbon catabolite repression. Microbiol. Mol. Biol. Rev. 62, 334–361.
Gancedo, J.M., Gancedo, C., 1971. Fructose-1, 6-diphosphatase, phosphofructokinase and glucose-6-phosphate dehydrogenase from fermenting and non fermenting yeasts. Arch. Microbiol. 138, 132–138.
Gardner, T.S., Hawkins, K.M., Meadows, A.L., Tsong, A.E., Tsegaye, Y., 2013. Production of acetyl-coenzyme A derived isoprenoids. WO2013071172A1.
Geertman, J.-M.A., Van Dijken, J.P., Pronk, J.T., 2006. Engineering NADH metabolism in *Saccharomyces cerevisiae*: Formate as an electron donor for glycerol production by anaerobic, glucose-limited chemostat cultures. FEMS Yeast Res. 6, 1193–1203.
Guadalupe-Medina, V., Wisselink, H.W., Luttik, M.A.H., De Hulster, E., Daran, J.-M., Pronk, J.T., Van Maris, A.J.A., 2013. Carbon dioxide fixation by Calvin-Cycle enzymes improves ethanol yield in yeast. Biotechnol. Biofuels 6, 125.
Hawkins, K.M., Mahatdejkul-Meadows, T.T., Meadows, A.L., Pickens, L.B., Tai, A., Tsong, A.E., 2014. Use of phosphoketolase and phosphotransacetylase for production of acetyl-coenzyme a derived compounds. WO2014144135A3.
Heath, E.C., Hurwitz, J., Horecker, B.L., Ginsburg, A., 1958. Pentose fermentation by *Lactobacillus plantarum*. I. The cleavage of xylulose 5-phosphate by phosphoketolase. J. Biol. Chem. 231, 1009–1029.
Heijnen, J.J., Van Loosdrecht, M.C.M., Tijhuis, L., 1992. A black box mathematical model to calculate auto- and heterotrophic biomass yields based on Gibbs energy dissipation. Biotechnol. Bioeng. 40, 1139–1154.
Henry, C.S., Broadbelt, L.J., Hatzimanikatis, V., 2007. Thermodynamics-based metabolic flux analysis. Biophys. J. 92, 1792–1805.
Hoelsch, K., Sührer, I., Heusel, M., Weuster-Botz, D., 2013. Engineering of formate dehydrogenase: Synergistic effect of mutations affecting cofactor specificity and chemical stability. Appl. Microbiol. Biotechnol. 97, 2473–2481.
Hughes, N.J., Clayton, C.L., Chalk, P.A., Kelly, D.J., 1998. *Helicobacter pylori porCDAB* and *oorDABC* genes encode distinct pyruvate:flavodoxin and 2-oxoglutarate: acceptor oxidoreductases which mediate electron transport to NADP. J. Bacteriol. 180, 1119–1128.
Huh, W.-K., Falvo, J.V., Gerke, L.C., Carroll, A.S., Howson, R.W., Weissman, J.S., O'Shea, E.K., 2003. Global analysis of protein localization in budding yeast. Nature 425, 686–691.
Inui, H., Miyatake, K., Nakano, Y., 1984a. Occurrence of oxygen-sensitive, $NADP^+$-dependent pyruvate dehydrogenase in mitochondria of *Euglena gracilis*. J. Biochem. 96, 931–934.
Inui, H., Miyatake, K., Nakano, Y., Kitaoka, S., 1984b. Fatty acid synthesis in mitochondria of *Euglena gracilis*. Eur. J. Biochem. 142, 121–126.
Inui, H., Yamaji, R., Saidoh, H., Nakano, Y., Kitaoka, S., 1991. Pyruvate:$NADP^+$ oxidoreductase from *Euglena gracilis*: limited proteolysis of the enzyme with trypsin. Arch. Biochem. Biophys. 286, 270–276.
Külzer, R., Pils, T., Kappl, R., Hüttermann, J., Knappe, J., 1998. Reconstitution and characterization of the polynuclear iron-sulfur cluster in pyruvate formate-lyase-activating enzyme. Molecular properties of the holoenzyme form. J. Biol. Chem. 273, 4897–4903.
Kandler, O., 1983. Carbohydrate metabolism in lactic acid bacteria. Antonie van Leeuwenhoek 49, 209–224.
Kanehisa, M., Goto, S., Sato, Y., Kawashima, M., Furumichi, M., Tanabe, M., 2014. Data, information, knowledge and principle: back to metabolism in KEGG. Nucleic Acids Res. 42, 199–205.
Khan, A., Kolattukudy, P.E., 1973. A microsomal fatty acid synthetase coupled to acyl-CoA reductase in *Euglena gracilis*. Arch. Biochem. Biophys. 158, 411–420.
Kispal, G., Cseko, J., Alkonyi, I., Sandor, A., 1991. Isolation and characterization of carnitine acetyltransferase from *S. cerevisiae*. Biochim. Biophys. Acta 1085, 217–222.
Knappe, J., Blaschkowski, H.P., Gröbner, P., Schmitt, T., 1974. Pyruvate formate-lyase of *Escherichia coli*: the acetyl-enzyme intermediate. Eur. J. Biochem. 50, 253–263.
Knappe, J., Schacht, J., Möckel, W., Höpner, T., Vetter, H., Edenharder, R., 1969. Pyruvate formate-lyase reaction in *Escherichia coli*. the enzymatic system converting an inactive form of the lyase into the catalytically active enzyme. Eur. J. Biochem. 11, 316–327.
Kocharin, K., Siewers, V., Nielsen, J., 2013. Improved polyhydroxybutyrate production by *Saccharomyces cerevisiae* through the use of the phosphoketolase pathway. Biotechnol. Bioeng. 110, 2216–2224.
Koh, J.L.Y., Chong, Y.T., Friesen, H., Moses, A., Boone, C., Andrews, B.J., Moffat, J., 2015. CYCLoPs: A comprehensive database constructed from automated analysis of protein abundance and subcellular localization patterns in *Saccharomyces cerevisiae*. G3 5, pp. 1223–1232.
Kohlhaw, G.B., Tan-Wilson, A., 1977. Carnitine acetyltransferase: Candidate for the transfer of acetyl groups through the mitochondrial membrane of yeast. J. Bacteriol. 129, 1159–1161.
Koike, M., Reed, L.J., Carroll, W.R., 1963. α-Keto acid dehydrogenation complexes. IV. Resolution and reconstitution of the *Escherichia coli* pyruvate dehydrogenation complex. J. Biol. Chem. 238, 30–39.
Koopman, F., Beekwilder, J., Crimi, B., Van Houwelingen, A., Hall, R.D., Bosch, D., Van Maris, A.J.A., Pronk, J.T., Daran, J.-M., 2012. *De novo* production of the flavonoid naringenin in engineered *Saccharomyces cerevisiae*. Microb. Cell. Fact. 11, 155.
Kozak, B.U., Van Rossum, H.M., Benjamin, K.R., Wu, L., Daran, J.-M.G., Pronk, J.T., Van Maris, A.J.A., 2014a. Replacement of the *Saccharomyces cerevisiae* acetyl-CoA synthetases by alternative pathways for cytosolic acetyl-CoA synthesis. Metab. Eng. 21, 46–59.
Kozak, B.U., Van Rossum, H.M., Niemeijer, M.S., Van Dijk, M., Benjamin, K., Wu, L., Daran, J.-M.G., Pronk, J.T., Van Maris, A.J.A., 2016. Replacement of the initial steps of ethanol metabolism in *Saccharomyces cerevisiae* by ATP-independent acetylating acetaldehyde dehydrogenase. FEMS Yeast Res. 16, fow006.
Kozak, B.U., Van Rossum, H.M., Luttik, M.A.H., Akeroyd, M., Benjamin, K.R., Wu, L., De Vries, S., Daran, J.-M., Pronk, J.T., Van Maris, A.J.A., 2014b. Engineering acetyl coenzyme A supply: Functional expression of a bacterial pyruvate dehydrogenase complex in the cytosol of *Saccharomyces cerevisiae*. mBio 5, e01696–14.
Krivoruchko, A., Serrano-Amatriain, C., Chen, Y., Siewers, V., Nielsen, J., 2013. Improving biobutanol production in engineered *Saccharomyces cerevisiae* by manipulation of acetyl-CoA metabolism. J. Ind. Microbiol. Biotechnol. 40, 1051–1056.
Krivoruchko, A., Zhang, Y., Siewers, V., Chen, Y., Nielsen, J., 2015. Microbial acetyl-CoA metabolism and metabolic engineering. Metab. Eng. 28, 28–42.
Leaf, T.A., Peterson, M.S., Stoup, S.K., Somers, D., Srienc, F., 1996. *Saccharomyces*

cerevisiae expressing bacterial polyhydroxybutyrate synthase produces poly-3-hydroxybutyrate. Microbiology 142, 1169–1180.
Lian, J., Zhao, H., 2015a. Recent advances in biosynthesis of fatty acids derived products in *Saccharomyces cerevisiae* via enhanced supply of precursor metabolites. J. Ind. Microbiol. Biotechnol. 42, 437–451.
Lian, J., Zhao, H., 2015b. Reversal of the β-oxidation cycle in *Saccharomyces cerevisiae* for production of fuels and chemicals. ACS Synth. Biol. 4, 332–341.
Lian, J., Si, T., Nair, N.U., Zhao, H., 2014. Design and construction of acetyl-CoA overproducing *Saccharomyces cerevisiae* strains. Metab. Eng. 24, 139–149.
Lipmann, F., 1940. A phosphorylated oxidation product of pyruvic acid. J. Biol. Chem. 134, 463–464.
Ljungdahl, L., Wood, H.G., 1969. Total synthesis of acetate from CO_2 by heterotrophic bacteria. Annu. Rev. Microbiol. 23, 515–538.
Lynd, L.R., Wyman, C.E., Gerngross, T.U., 1999. Biocommodity engineering. Biotechnol. Prog. 15, 777–793.
Mainguet, S.E., Gronenberg, L.S., Wong, S.S., Liao, J.C., 2013. A reverse glyoxylate shunt to build a non-native route from C4 to C2 in *Escherichia coli*. Metab. Eng. 19, 116–127.
Mascal, M., 2012. Chemicals from biobutanol: technologies and markets. Biofuels, Bioprod. Bioref. 6, 483–493.
Max, B., Salgado, J.M., Rodríguez, N., Cortés, S., Converti, A., Domínguez, J.M., 2010. Biotechnological production of citric acid. Braz. J. Microbiol. 41, 862–875.
McIver, L., Leadbeater, C., Campopiano, D.J., Baxter, R.L., Daff, S.N., Chapman, S.K., Munro, A.W., 1998. Characterisation of flavodoxin $NADP^+$ oxidoreductase and flavodoxin; key components of electron transfer in *Escherichia coli*. Eur. J. Biochem. 257, 577–585.
Melnikov, S., Ben-Shem, A., Garreau de Loubresse, N., Jenner, L., Yusupova, G., Yusupov, M., 2012. One core, two shells: bacterial and eukaryotic ribosomes. Nat. Struct. Mol. Biol. 19, 560–567.
Miller, C., Fosmer, A., Rush, B., McMullin, T., Beacom, D., Suominen, P., 2011. Industrial production of lactic acid. Compr. Biotechnol., 179–188.
Navas, M. a, Gancedo, J.M., 1996. The regulatory characteristics of yeast fructose-1,6-bisphosphatase confer only a small selective advantage. J. Bacteriol. 178, 1809–1812.
Nielsen, J., 2014. Synthetic biology for engineering acetyl coenzyme A metabolism in yeast. MBio 5, e02153.
Nielsen, J., Larsson, C., Van Maris, A.J.A., Pronk, J.T., 2013. Metabolic engineering of yeast for production of fuels and chemicals. Curr. Opin. Biotechnol. 24, 398–404.
Nielsen, J., Siewers, V., Kirvoruchko, A., Zhang, Y., Zhou, Y., Buds, N.A.A., Dai, Z., 2015. Engineering of acetyl-CoA metabolism in yeast. WO2015057154 A3.
Noor, E., Haraldsdóttir, H.S., Milo, R., Fleming, R.M.T., 2013. Consistent estimation of Gibbs energy using component contributions. PLoS Comput. Biol. 9, e1003098.
Oud, B., Flores, C.-L., Gancedo, C., Zhang, X., Trueheart, J., Daran, J.-M., Pronk, J.T., Van Maris, A.J.A., 2012. An internal deletion in *MTH1* enables growth on glucose of pyruvate-decarboxylase negative, non-fermentative *Saccharomyces cerevisiae*. Microb. Cell. Fact. 11, 131.
Oura, E., 1972. The Effect of Aeration on the Growth Energetics and Biochemical Composition of Baker's Yeast. University of Helsinki, Finland.
Overkamp, K.M., Kötter, P., Van der Hoek, R., Schoondermark-Stolk, S., Luttik, Ma. H., Van Dijken, J.P., Pronk, J.T., 2002. Functional analysis of structural genes for NAD(+)-dependent formate dehydrogenase in *Saccharomyces cerevisiae*. Yeast 19, 509–520.
Paddon, C.J., Westfall, P.J., Pitera, D.J., Benjamin, K., Fisher, K., McPhee, D., Leavell, M. D., Tai, A., Main, A., Eng, D., Polichuk, D.R., Teoh, K.H., Reed, D.W., Treynor, T., Lenihan, J., Fleck, M., Bajad, S., Dang, G., Dengrove, D., Diola, D., Dorin, G., Ellens, K.W., Fickes, S., Galazzo, J., Gaucher, S.P., Geistlinger, T., Henry, R., Hepp, M., Horning, T., Iqbal, T., Jiang, H., Kizer, L., Lieu, B., Melis, D., Moss, N., Regentin, R., Secrest, S., Tsuruta, H., Vazquez, R., Westblade, L.F., Xu, L., Yu, M., Zhang, Y., Zhao, L., Lievense, J., Covello, P.S., Keasling, J.D., Reiling, K.K., Renninger, N.S., Newman, J.D., 2013. High-level semi-synthetic production of the potent antimalarial artemisinin. Nature 496, 528–532.
Palmieri, L., Lasorsa, F.M., Iacobazzi, V., Runswick, M.J., Palmieri, F., Walker, J.E., 1999. Identification of the mitochondrial carnitine carrier in *Saccharomyces cerevisiae*. FEBS Lett. 462, 472–476.
Pel, H.J., De Winde, J.H., Archer, D.B., Dyer, P.S., Hofmann, G., Schaap, P.J., Turner, G., De Vries, R.P., Albang, R., Albermann, K., Andersen, M.R., Bendtsen, J.D., Benen, Ja. E., Van den Berg, M., Breestraat, S., Caddick, M.X., Contreras, R., Cornell, M., Coutinho, P.M., Danchin, E.G.J., Debets, A.J.M., Dekker, P., Van Dijck, P.W.M., Van Dijk, A., Dijkhuizen, L., Driessen, A.J.M., D'Enfert, C., Geysens, S., Goosen, C., Groot, G.S.P., De Groot, P.W.J., Guillemette, T., Henrissat, B., Herweijer, M., Van den Hombergh, J.P.T.W., Van den Hondel, C.A.M.J.J., Van der Heijden, R.T.J.M., Van der Kaaij, R.M., Klis, F.M., Kools, H.J., Kubicek, C.P., Van Kuyk, P.A., Lauber, J., Lu, X., Van der Maarel, M.J.E.C., Meulenberg, R., Menke, H., Mortimer, M.A., Nielsen, J., Oliver, S.G., Olsthoorn, M., Pal, K., Van Peij, N.N.M.E., Ram, A.F.J., Rinas, U., Roubos, J.A., Sagt, C.M.J., Schmoll, M., Sun, J., Ussery, D., Varga, J., Vervecken, W., Van de Vondervoort, P.J.J., Wedler, H., Wösten, H.A.B., Zeng, A.-P., Van Ooyen, A.J.J., Visser, J., Stam, H., 2007. Genome sequencing and analysis of the versatile cell factory *Aspergillus niger* CBS 513.88. Nat. Biotechnol. 25, 221–231.
Pokholok, D.K., Harbison, C.T., Levine, S., Cole, M., Hannett, N.M., Lee, T.I., Bell, G.W., Walker, K., Rolfe, P.A., Herbolsheimer, E., Zeitlinger, J., Lewitter, F., Gifford, D.K., Young, R.A., 2005. Genome-wide map of nucleosome acetylation and methylation in yeast. Cell 122, 517–527.
Porro, D., Brambilla, L., Ranzi, B.M., Martegani, E., Alberghina, L., 1995. Development of metabolically engineered *Saccharomyces cerevisiae* cells for the production of lactic acid. Biotechnol. Prog. 11, 294–298.
Pronk, J.T., Steensma, H.Y., Van Dijken, J.P., 1996. Pyruvate metabolism in *Saccharomyces cerevisiae*. Yeast 12, 1607–1633.
Pronk, J.T., Wenzel, T.J., Luttik, M.A., Klaassen, C.C., Scheffers, W.A., Steensma, H.Y., Van Dijken, J.P., 1994. Energetic aspects of glucose metabolism in a pyruvate-dehydrogenase-negative mutant of *Saccharomyces cerevisiae*. Microbiology 140, 601–610.
Przybyla-Zawislak, B., Dennis, R.A., Zakharkin, S.O., McCammon, M.T., 1998. Genes of succinyl-CoA ligase from *Saccharomyces cerevisiae*. Eur. J. Biochem. 258, 736–743.
Ragsdale, S.W., 2003. Pyruvate ferredoxin oxidoreductase and its radical intermediate. Chem. Rev. 103, 2333–2346.
Ratledge, C., Holdsworth, J., 1985. Properties of a pentulose-5-phosphate phosphoketolase from yeasts grown on xylose. Appl. Microbiol. Biotechnol. 22, 217–221.
Rodriguez, S., Denby, C.M., Van Vu, T., Baidoo, E.E.K., Wang, G., Keasling, J.D., 2016. ATP citrate lyase mediated cytosolic acetyl-CoA biosynthesis increases mevalonate production in *Saccharomyces cerevisiae*. Microb. Cell. Fact. 15, 48.
Rotte, C., Stejskal, F., Zhu, G., Keithly, J.S., Martin, W., 2001. Pyruvate:$NADP^+$ oxidoreductase from the mitochondrion of *Euglena gracilis* and from the apicomplexan *Cryptosporidium parvum*: a biochemical relic linking pyruvate metabolism in mitochondriate and amitochondriate protists. Mol. Biol. Evol. 18, 710–720.
Rude, M.A., Schirmer, A., 2009. New microbial fuels: a biotech perspective. Curr. Opin. Microbiol. 12, 274–281.
Ruijter, G.J.G., Panneman, H., Xu, D.B., Visser, J., 2000. Properties of *Aspergillus niger* citrate synthase and effects of citA overexpression on citric acid production. FEMS Microbiol. Lett. 184, 35–40.
Ruiz-Amil, M., De Torrontegui, G., Palacián, E., Catalina, L., Losada, M., 1965. Properties and function of yeast pyruvate carboxylase. J. Biol. Chem. 240, 3485–3492.
Sánchez, B.J., Nielsen, J., 2015. Genome scale models of yeast: Towards standardized evaluation and consistent omic integration. Integr. Biol. 7, 846–858.
Salusjarvi, L., Kaunisto, S., Holmstrom, S., Vehkomaki, M.L., Koivuranta, K., Pitkanen, J.P., Ruohonen, L., 2013. Overexpression of NADH-dependent fumarate reductase improves D-xylose fermentation in recombinant *Saccharomyces cerevisiae*. J. Ind. Microbiol. Biotechnol. 40, 1383–1392.
Sandoval, C.M., Ayson, M., Moss, N., Lieu, B., Jackson, P., Gaucher, S.P., Horning, T., Dahl, R.H., Denery, J.R., Abbott, D.A., Meadows, A.L., 2014. Use of pantothenate as a metabolic switch increases the genetic stability of farnesene producing *Saccharomyces cerevisiae*. Metab. Eng. 25, 1–12.
Sawers, R.G., 1994. The hydrogenases and formate dehydrogenases of *Escherichia coli*. Antonie van Leeuwenhoek 66, 57–88.
Schmalix, W., Bandlow, W., 1993. The ethanol-inducible *YAT1* gene from yeast encodes a presumptive mitochondrial outer carnitine acetyltransferase. J. Biol. Chem. 268, 27428–27439.
Schramm, M., Racker, E., 1957. Formation of erythrose-4-phosphate and acetyl phosphate by a phosphorolytic cleavage of fructose-6-phosphate. Nature 179, 1349–1350.
Schramm, M., Klybas, V., Racker, E., 1958. Phosphorolytic cleavage of fructose-6-phosphate by fructose-6-phosphate phosphoketolase from *Acetobacter xylinum*. J. Biol. Chem. 233, 1283–1288.
Schuchmann, K., Müller, V., 2014. Autotrophy at the thermodynamic limit of life: a model for energy conservation in acetogenic bacteria. Nat. Rev. Microbiol. 12, 809–821.
Serov, A.E., Popova, A.S., Fedorchuk, V.V., Tishkov, V.I., 2002. Engineering of coenzyme specificity of formate dehydrogenase from *Saccharomyces cerevisiae*. Biochem. J. 367, 841–847.
Sheng, J., Feng, X., 2015. Metabolic engineering of yeast to produce fatty acid-derived biofuels: bottlenecks and solutions. Front. Microbiol. 6, 1–11.
Shiba, Y., Paradise, E.M., Kirby, J., Ro, D.-K., Keasling, J.D., 2007. Engineering of the pyruvate dehydrogenase bypass in *Saccharomyces cerevisiae* for high-level production of isoprenoids. Metab. Eng. 9, 160–168.
Snoep, J.L., Westphal, A.H., Benen, J.A.E., Teixeira de Mattos, M.J., Neijssel, O.M., Kok, A., 1992. Isolation and characterisation of the pyruvate dehydrogenase complex of anaerobically grown *Enterococcus faecalis* NCTC 775. Eur. J. Biochem. 203, 245–250.
Snoep, J.L., De Graef, M.R., Westphal, A.H., De Kok, A., Teixeira de Mattos, M.J., Neijssel, O.M., 1993. Differences in sensitivity to NADH of purified pyruvate dehydrogenase complexes of *Enterococcus faecalis*, *Lactococcus lactis*, *Azotobacter vinelandii* and *Escherichia coli*: Implications for their activity *in vivo*. FEMS Microbiol. Lett. 114, 279–283.
Soh, K.C., Miskovic, L., Hatzimanikatis, V., 2012. From network models to network responses: integration of thermodynamic and kinetic properties of yeast genome-scale metabolic networks. FEMS Yeast Res. 12, 129–143.
Sonderegger, M., Schümperli, M., Sauer, U., 2004. Metabolic engineering of a phosphoketolase pathway for pentose catabolism in *Saccharomyces cerevisiae*. Appl. Environ. Microbiol. 70, 2892–2897.
Stadtman, E.R., 1952. The purification and properties of phosphotransacetylase. J. Biol. Chem. 196, 527–534.
Stairs, C.W., Roger, A.J., Hampl, V., 2011. Eukaryotic pyruvate formate lyase and its activating enzyme were acquired laterally from a firmicute. Mol. Biol. Evol. 28, 2087–2099.
Steen, E.J., Chan, R., Prasad, N., Myers, S., Petzold, C.J., Redding, A., Ouellet, M., Keasling, J.D., 2008. Metabolic engineering of *Saccharomyces cerevisiae* for the production of *n*-butanol. Microb. Cell. Fact. 7, 36.
Strijbis, K., Van Roermund, C.W.T., Hardy, G.P., Van den Burg, J., Bloem, K., De Haan, J., Van Vlies, N., Wanders, R.J.A., Vaz, F.M., Distel, B., 2009. Identification and

characterization of a complete carnitine biosynthesis pathway in *Candida albicans*. FASEB J. 23, 2349–2359.
Sutendra, G., Kinnaird, A., Dromparis, P., Paulin, R., Stenson, T.H., Haromy, A., Hashimoto, K., Zhang, N., Flaim, E., Michelakis, E.D., 2014. A nuclear pyruvate dehydrogenase complex is important for the generation of acetyl-CoA and histone acetylation. Cell 158, 84–97.
Swidah, R., Wang, H., Reid, P.J., Ahmed, H.Z., Pisanelli, A.M., Persaud, K.C., Grant, C. M., Ashe, M.P., 2015. Butanol production in *S. cerevisiae* via a synthetic ABE pathway is enhanced by specific metabolic engineering and butanol resistance. Biotechnol. Biofuels 8, 97.
Swiegers, J.H., Dippenaar, N., Pretorius, I.S., Bauer, F.F., 2001. Carnitine-dependent metabolic activities in *Saccharomyces cerevisiae*: three carnitine acetyltransferases are essential in a carnitine-dependent strain. Yeast 18, 585–595.
Tang, X., Feng, H., Chen, W.N., 2013. Metabolic engineering for enhanced fatty acids synthesis in *Saccharomyces cerevisiae*. Metab. Eng. 16, 95–102.
Tehlivets, O., Scheuringer, K., Kohlwein, S.D., 2007. Fatty acid synthesis and elongation in yeast. Biochim. Biophys. Acta 1771, 255–270.
Thykaer, J., Nielsen, J., 2007. Evidence, through C13-labelling analysis, of phosphoketolase activity in fungi. Process. Biochem. 42, 1050–1055.
Tittmann, K., Wille, G., Golbik, R., Weidner, A., Ghisla, S., Hübner, G., 2005. Radical phosphate transfer mechanism for the thiamin diphosphate- and FAD-dependent pyruvate oxidase from *Lactobacillus plantarum*. Kinetic coupling of intercofactor electron transfer with phosphate transfer to acetyl-thiamin diphosphate via a trans. Biochemistry 44, 13291–13303.
Tucci, S., Vacula, R., Krajcovic, J., Proksch, P., Martin, W., 2010. Variability of wax ester fermentation in natural and bleached *Euglena gracilis* strains in response to oxygen and the elongase inhibitor flufenacet. J. Eukaryot. Microbiol. 57, 63–69.
Van den Berg, M.A., Steensma, H.Y., 1995. *ACS2*, a *Saccharomyces cerevisiae* gene encoding acetyl-coenzyme A synthetase, essential for growth on glucose. Eur. J. Biochem. 231, 704–713.
Van Maris, A.J.A., Luttik, M.A.H., Winkler, A.A., Van Dijken, J.P., Pronk, J.T., 2003. Overproduction of threonine aldolase circumvents the biosynthetic role of pyruvate decarboxylase in glucose-limited chemostat cultures of *Saccharomyces cerevisiae*. Appl. Environ. Microbiol. 69, 2094–2099.
Van Maris, A.J.A., Winkler, A.A., Porro, D., Van Dijken, J.P., Pronk, J.T., 2004b. Homofermentative lactate production cannot sustain anaerobic growth of engineered *Saccharomyces cerevisiae*: possible consequence of energy-dependent lactate export. Appl. Environ. Microbiol. 70, 2898–2905.
Van Maris, A.J.A., Geertman, J.A., Vermeulen, A., Groothuizen, M.K., Winkler, A.A., Piper, M.D.W., Van Dijken, J.P., Pronk, J.T., 2004a. Directed evolution of pyruvate decarboxylase-negative *Saccharomyces cerevisiae*, yielding a C_2-independent, glucose-tolerant, and pyruvate-hyperproducing yeast. Appl. Environ. Microbiol. 70, 159–166.
Van Roermund, C.W., Elgersma, Y., Singh, N., Wanders, R.J., Tabak, H.F., 1995. The membrane of peroxisomes in *Saccharomyces cerevisiae* is impermeable to NAD (H) and acetyl-CoA under *in vivo* conditions. EMBO J. 14, 3480–3486.
Van Roermund, C.W., Hettema, E.H., Van den Berg, M., Tabak, H.F., Wanders, R.J., 1999. Molecular characterization of carnitine-dependent transport of acetyl-CoA from peroxisomes to mitochondria in *Saccharomyces cerevisiae* and identification of a plasma membrane carnitine transporter, Agp2p. EMBO J. 18, 5843–5852.
Van Rossum, H.M., Kozak, B.U., Niemeijer, M.S., Duine, H.J., Luttik, M.A.H., Boer, V. M., Kötter, P., Daran, J.-M.G., Van Maris, A.J.A., Pronk, J.T., 2016a. Alternative reactions at the interface of glycolysis and citric acid cycle in *Saccharomyces cerevisiae*. FEMS Yeast Res., fow017
Van Rossum, H.M., Kozak, B.U., Niemeijer, M.S., Dykstra, J.C., Luttik, M.A.H., Daran, J.-M.G., Van Maris, A.J.A., Pronk, J.T., 2016b. Requirements for carnitine-shuttle-mediated translocation of mitochondrial acetyl moieties to the yeast cytosol. (Unpublished results).
Vax, F.M., Wanders, R.J.A., 2002. Carnitine biosynthesis in mammals. Biochem. J. 361, 417.
Verduyn, C., Stouthamer, A.H, Scheffers, W.A, Van Dijken, J.P, 1991. A theoretical evaluation of growth yields of yeasts Antonie van Leeuwenhoek 59, 49–63.
Verwaal, R., Wang, J., Meijnen, J.P., Visser, H., Sandmann, G., Van Den Berg, J.A., Van Ooyen, A.J.J., 2007. High-level production of beta-carotene in *Saccharomyces cerevisiae* by successive transformation with carotenogenic genes from *Xanthophyllomyces dendrorhous*. Appl. Environ. Microbiol. 73, 4342–4350.
Von Kamp, A., Schuster, S., 2006. Metatool 5.0: fast and flexible elementary modes analysis. Bioinformatics 22, 1930–1931.
Waks, Z., Silver, P.A., 2009. Engineering a synthetic dual-organism system for hydrogen production. Appl. Environ. Microbiol. 75, 1867–1875.
Weusthuis, R.A., Lamot, I., Van der Oost, J., Sanders, J.P.M., 2011. Microbial production of bulk chemicals: Development of anaerobic processes. Trends Biotechnol. 29, 153–158.
Yan, D., Wang, C., Zhou, J., Liu, Y., Yang, M., Xing, J., 2014. Construction of reductive pathway in *Saccharomyces cerevisiae* for effective succinic acid fermentation at low pH value. Bioresour. Technol. 156, 232–239.
Zelle, R.M., De Hulster, E., Van Winden, W.A., De Waard, P., Dijkema, C., Winkler, A. A., Geertman, J.-M.A., Van Dijken, J.P., Pronk, J.T., Van Maris, A.J.A., 2008. Malic acid production by *Saccharomyces cerevisiae*: engineering of pyruvate carboxylation, oxaloacetate reduction, and malate export. Appl. Environ. Microbiol. 74, 2766–2777.
Zhang, J., Pierick, A., ten, Van Rossum, H.M., Maleki Seifar, R., Ras, C., Daran, J.-M., Heijnen, J.J., Aljoscha Wahl, S., 2015a. Determination of the cytosolic NADPH/NADP ratio in *Saccharomyces cerevisiae* using shikimate dehydrogenase as sensor reaction. Sci. Rep. 5, 12846.
Zhang, Y., Dai, Z., Krivoruchko, A., Chen, Y., Siewers, V., Nielsen, J., 2015b. Functional pyruvate formate lyase pathway expressed with two different electron donors in *Saccharomyces cerevisiae* at aerobic growth. FEMS Yeast Res. 15, fov024.
Zhou, Z.H., McCarthy, D.B., O'Connor, C.M., Reed, L.J., Stoops, J.K., 2001. The remarkable structural and functional organization of the eukaryotic pyruvate dehydrogenase complexes. Proc. Natl. Acad. Sci. USA 98, 14802–14807.